AD A124 960 MODULAR INCOHERENT CO2 TEA LASERS(U) RAYTHEON CO 1/1
SUDBURY MA ELECTRO-OPTICS SYSTEMS LAB
J T GANLEY ET AL. 10 SEP 82 ER82-4284 DAAK70-80-C-0090
UNCLASSIFIED F/G 20/5 . NL

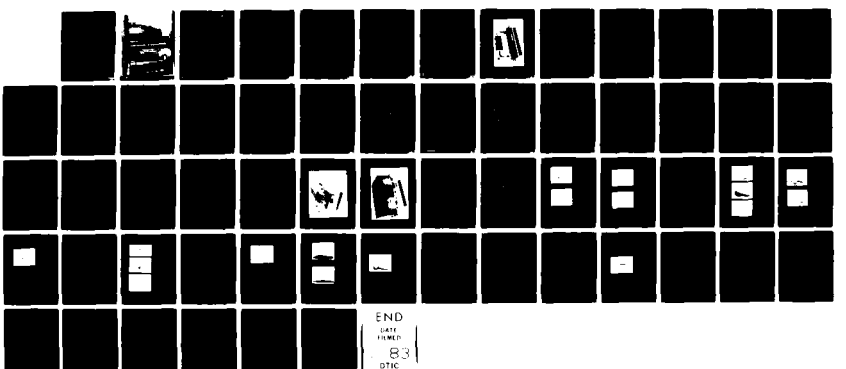

END
DATE FILMED
83
DTIC

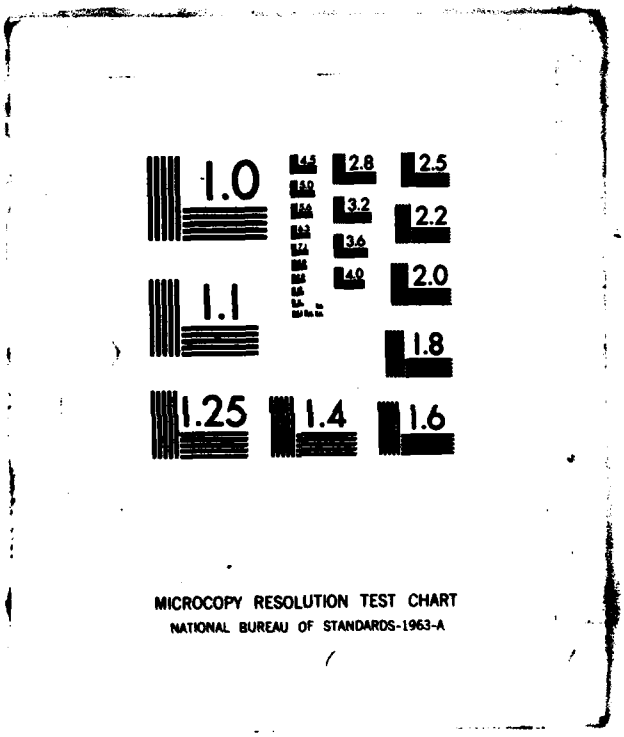

MICROCOPY RESOLUTION TEST CHART
NATIONAL BUREAU OF STANDARDS-1963-A

UNCLASSIFIED

SECURITY CLASSIFICATION OF THIS PAGE (When Data Entered)

REPORT DOCUMENTATION PAGE		READ INSTRUCTIONS BEFORE COMPLETING FORM
1. REPORT NUMBER	2. GOVT ACCESSION NO. AD-A124760	3. RECIPIENT'S CATALOG NUMBER
4. TITLE (and Subtitle) Modular Incoherent CO_2 TEA Lasers Final Report		5. TYPE OF REPORT & PERIOD COVERED Final Report 7/15/80 - 8/31/82
		6. PERFORMING ORG. REPORT NUMBER ER82-4284
7. AUTHOR(s) J. T. Ganley A. J. Legere		8. CONTRACT OR GRANT NUMBER(s) DAAK70-80-C-0090
9. PERFORMING ORGANIZATION NAME AND ADDRESS RAYTHEON COMPANY Electro-Optics Systems Laboratory 528 Boston Post Road, Sudbury, MA 01776		10. PROGRAM ELEMENT, PROJECT, TASK AREA & WORK UNIT NUMBERS
11. CONTROLLING OFFICE NAME AND ADDRESS U.S. ARMY ELECTRONICS RESEARCH & DEVELOPMENT COMMAND, Night Vision and Electro-Optics Lab. Fort Belvoir, VA 22060		12. REPORT DATE 10 September 1982
		13. NUMBER OF PAGES 54
14. MONITORING AGENCY NAME & ADDRESS(if different from Controlling Office)		15. SECURITY CLASS. (of this report) UNCLASSIFIED
		15a. DECLASSIFICATION/DOWNGRADING SCHEDULE

16. DISTRIBUTION STATEMENT (of this Report)
Approved for public release; distribution unlimited.

17. DISTRIBUTION STATEMENT (of the abstract entered in Block 20, if different from Report)

18. SUPPLEMENTARY NOTES

19. KEY WORDS (Continue on reverse side if necessary and identify by block number)
Incoherent TEA laser, cross-wind sensor, target designator, L-C inversion generator, plexiglass laser, alumina laser, voltage-doubling circuit, plus-minus charge circuitry, energy storage capacitors, high voltage blocking capacitors, trigger transformers, spark gap switches, high voltage charging supplies

20. ABSTRACT (Continue on reverse side if necessary and identify by block number)
Two pulsed 10-micron transmitter systems were designed, fabricated and tested, one for use in cross-wind sensor applications, and one for target designator applications. The goal of the Incoherent TEA laser effort was to make these units capable of the required optical and electrical performance characteristics with total system lifetimes of a few million pulses.

DD FORM 1 JAN 73 1473 EDITION OF 1 NOV 65 IS OBSOLETE

UNCLASSIFIED

SECURITY CLASSIFICATION OF THIS PAGE (When Data Entered)

TABLE OF CONTENTS

LIST OF ILLUSTRATIONS

SECTION 1

BACKGROUND

The purpose of the Incoherent TEA Laser effort is to provide two pulsed 10-micron transmitter systems. One of the systems, Unit A, is for use in target designator applications and the other, Unit B, is for use in cross-wind sensor applications. The general specifications of the contract require that Unit A be operated at repetition rates from 0 to 20 hertz, with output energy of at least 150 millijoules in a 60-nanosecond spike. Unit B is to be capable of producing pairs of laser pulses, with an interpulse time interval variable from 100 microseconds to 1 millisecond. Repetition rate is to be from 0 to 10 hertz with 75 millijoules in each of the pulses. Both units require circular polarization, TEM_{00} mode output, collimating optics, and sealed-off laser operation.

Figure 1 is a photograph of a Raytheon TEA laser of the type used in both target designator and cross-wind sensor applications. The laser consists of two separate discharge sections joined by a folded optical cavity. In designator applications, both discharges are fired simultaneously and a single laser pulse is obtained. For cross-wind sensor applications, the discharge sections are pulsed sequentially and two laser pulses are extracted.

During the initial design phase, several different designs were considered, and a design which involved machining the laser body from high alumina ceramic was chosen. Sealing parts to form a vacuum-tight assembly was to be done with the high temperature oven brazes and heliarc welds.

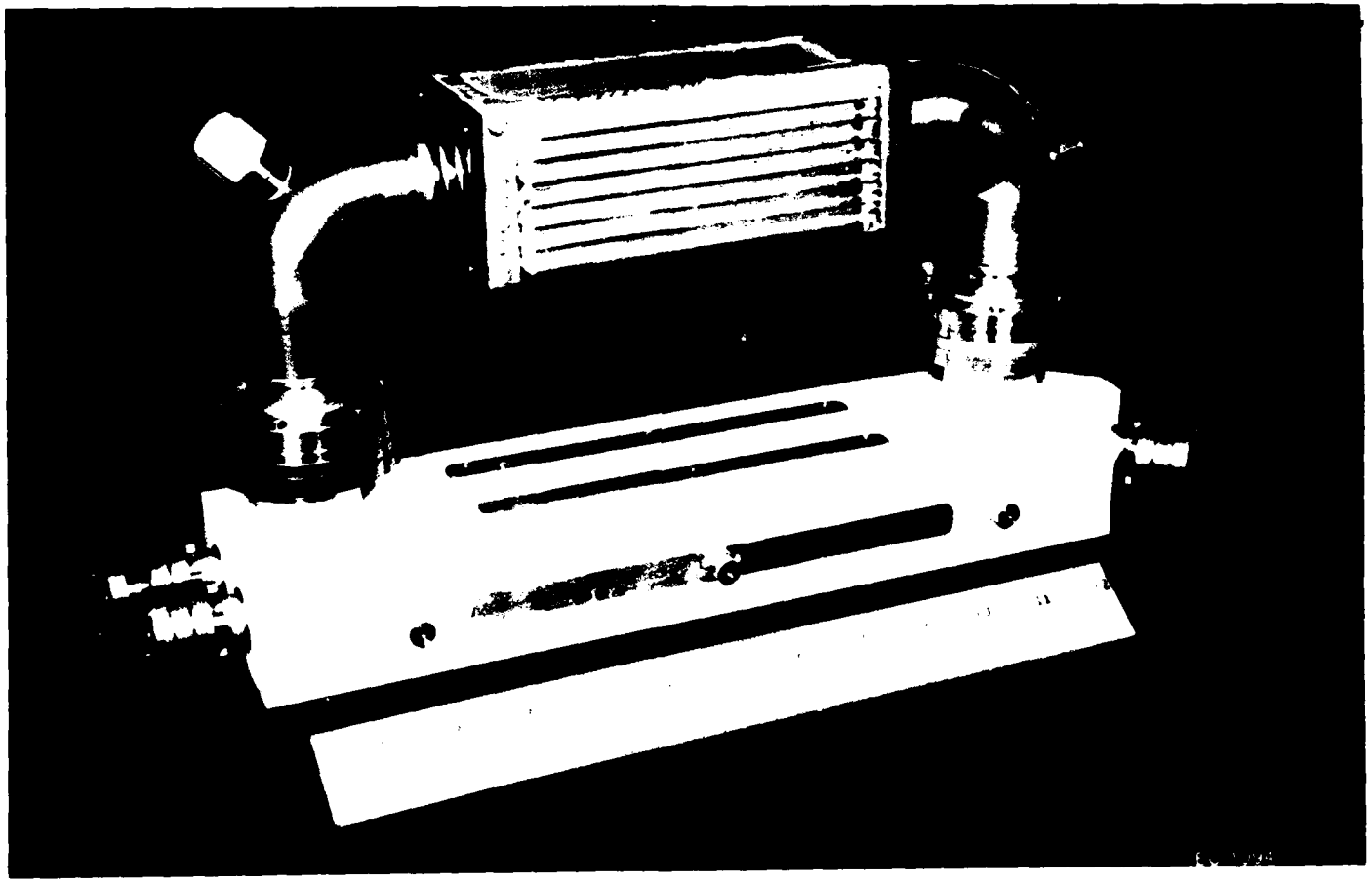

Figure 1. Raytheon Cross-Wind Sensor Laser

Each of the two transmitter units was to be supplied with its own power conditioning circuitry. The electrical circuitry required to drive a laser of the type shown in Figure 1 must perform a number of related tasks in a reliable manner. First, the pulser circuitry must store a quantity of electrical energy which is appropriate for producing the required optical output. For the Raytheon cross-wind sensor and designator lasers, which were previously driven by a rather inefficient L-C inversion generator, the energy storage requirements were roughly 6-8 joules per pulse for each of the two discharge sections. As will be discussed later, it has been possible to decrease this figure by more than a factor of two as a result of improved coupling of the pulser to the discharge load.

In addition to energy storage requirements, the pulser must deliver energy to the laser load at a voltage which will produce rapid and uniform breakdown of the laser gas. Typically 25 kV is required for the Raytheon lasers being discussed here, although operation as low as 18 kV or as high as 28 kV is possible under certain conditions.

The electrical circuitry must deliver energy to the laser load in a time less than a few hundred nanoseconds in order to avoid the formation of arcs in the discharge volume. Generally speaking, shorter electrical pulses are associated with more reliable laser operation. However, the higher currents associated with shorter pulses can shorten the lifetime of storage capacitors and switches in the pulser circuitry.

The ultimate goal of the Incoherent TEA Laser effort was to fabricate transmitter units capable of the required ootical and electrical performance characteristics, with total system lifetimes of a few million pulses. A number of problems were anticipated at the initiation of the work, the major one being the fabrication and operation of an alumina laser body with metalized seals. In addition to problems related to the laser, it was apparent that there would be a number of special problems with the electrical circuitry. Some customized

components would be required to allow for packaging the units in a reasonable volume. Also problems were anticipated in controlling electrical noise generated by firing the pulsers. Since the cross-wind sensor module must produce two pulses spaced by a definite time interval, it was anticipated that spurious triggering of the second pulser by noise generated in firing the first pulser would be a problem.

Previous experience has shown that one of the most serious problems with units of this type is the relatively short useful life of many of the high voltage components. Switches, capacitors, and charging supplies cannot survive for millions of pulses under such demanding conditions unless great care is exercised in both circuit design and component selection.

The Raytheon view of the anticipated work was that units with the required lifetime and electrical performance characteristics could be fabricated using modifications of existing components. It was our opinion that most of the problems associated with pulsers of the type being considered have resulted from improper circuit design and poor circuit layout rather than inadequate components. With this position as a starting point, the following electrical design decisions were made:

1) The unit would be fabricated as three interconnected sections, each housed in a separate metal enclosure. The three sections would include a low voltage logic control section, a high voltage charging and triggering section, and a high voltage energy storage and switching section. The metallic enclosures would be fabricated as an aluminum casting. This fabrication technique was chosen in order to shield the various circuit elements from electrical noise generated in other parts of the circuit.

2) Logic-controlled charging supplies with internal electronic ballasting would be used. Electronic ballasting eliminates the 50% energy loss which occurs with resistive ballasting. External logic control allows

for disabling the power supply while the energy storage capacitors are being fired. This protects the power supplies from transients and increases spark gap lifetime.

3) Advanced design spark gap switches would be considered, but standard gaps would be purchased as a backup. It was felt that standard gaps were available which could satisfy the lifetime requirements, but additional useful information might be gained by looking at alternative designs.

SECTION 2
LASER DESIGN AND FABRICATION

Early in the program, a decision was made to fabricate the lasers from high alumina ceramic and to use metalized seals. The laser would contain two discharge sections, isolated by a ceramic wall, and joined by a folded optical cavity. A single flow loop, containing a heat exchanger and a blower, would circulate gas through both discharge regions. A cross section of the laser and the flow loop is shown in Figure 2. Each discharge section is preionized by a single array of flashboard buttons. This single-sided illumination produces a spatially non-uniform electron density which is, for some conditions, adequate for initiation of a uniform glow discharge.

The overall dimensions of the laser body were determined by the maximum size of alumina block which could be fused and brazed within the ovens of Raytheon's Microwave and Power Tube Division. As can be seen from Figure 2, the machining of the laser block is an elaborate task, with exacting tolerances required on the surfaces which support the electrode and the mirror holders.

As work on the laser bodies proceeded, it became apparent that the fabrication task was more difficult than anticipated. Several steps were involved in the process because 3" x 2" x 16" blocks, necessary for fabricating the laser, were not routinely available. During the fusing operation, two sets of blocks were cracked during trial runs. Eventually, a total of 5 blocks, each 3" x 2" x 16", were sucessfully fabricated. The next step in the fabrication process was to fuse on the side arms for attaching the flow-loop flanges. Another block was lost due to cracking in this operation. Attempts were then made to machine the remaining four blocks. Two of these blocks were machined inaccurately with the remaining two blocks assembled as lasers. A number of companies were consulted regarding the metalizing and brazing job, but none would guarantee that the laser could be assembled without destroying them. As a result of these conversations, it was decided to assemble the lasers with epoxy rather than to risk the possible loss of the remaining two blocks.

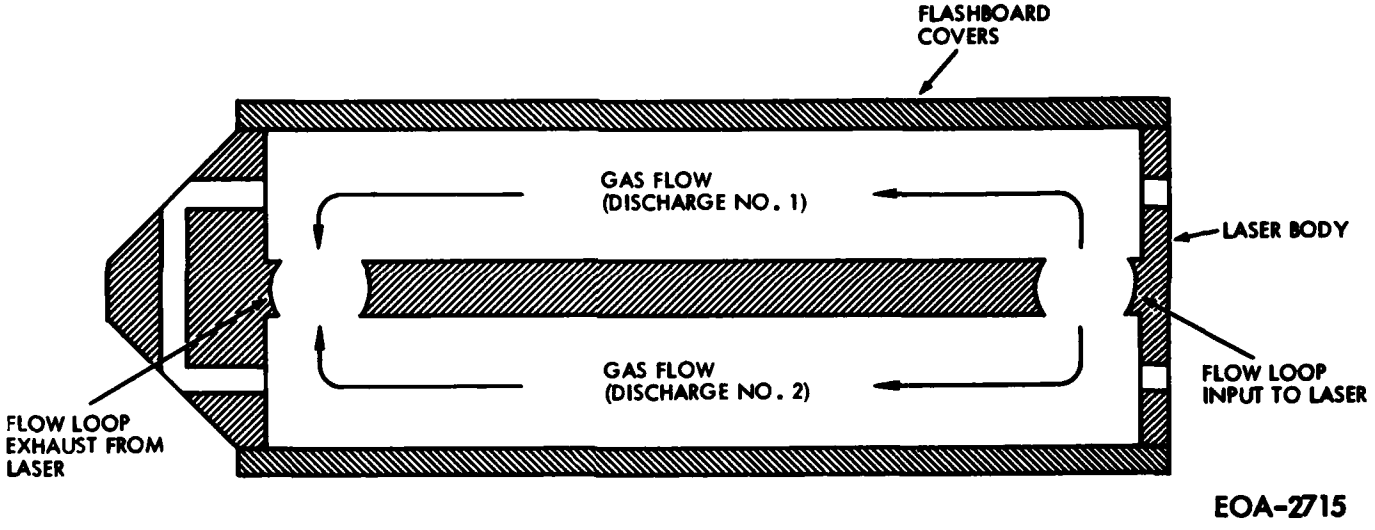

Figure 2. Schematic of Cross-Sectional View of Laser Body and Flow Loop Attachments

During an extensive trial period, both lasers were operated with temporary gasket seals on the flashboard covers. This allowed for disassembly of the laser and adjustment of the main electrodes and flashboards.

Optimum gas mixes, coupling efficiencies, mirror radii and input energies were determined during these tests. Tests were performed first with a plexiglass body laser and the data derived from this work were used as a starting point for experiments with the alumina body lasers.

The results of experiments with the plexiglass laser are summarized below:

1. It was determined that use of the L-C Inversion Generator-type circuit was very inefficient at driving the laser and led to very short life of some of the critical circuit components. A number of other circuits were tested with much better results. These tests will be discussed later.
2. Uniform discharges were obtained with the main electrodes canted by .008".
3. With proper coupling of the electrical circuit to the gas discharge load, the plexiglass laser provided 250 millijoules output, with only 6 joules input.
4. Best laser performance was achieved with a 5-meter radius copper end reflector and a 65% reflecting output flat. Good mode control was achieved with a .300" diameter mode-limiting aperture. Optimum gas mix for this laser was 20% CO_2, 10% N_2, and 70% He, and reliable operation with this mix was achieved with roughly 23 kV applied to the laser.

The experiments performed with the plexiglass laser were repeated with both the cross-wind sensor laser and the designator laser as soon as they were fabricated. The alumina lasers produced similar results with respect to voltage requirements and

electrode alignment tolerances. However, the output energy of each alumina unit was down significantly from the output of the plexiglass unit. This was due, in part, to inaccuracies in machining the alumina blocks where the holes bored at each end of the laser to join the mirrors to the discharge volume were not coplanar. This resulted in shadowing of part of the mode volume by the holes at the turnaround end of the laser.

As a result of the tests performed while the lasers were assembled with gasket seals, the following design decisions were made:

1. Electrode spacing - .340"
2. Electrode cant - .008"
3. Discharge voltage - 22.5 kV
4. Energy storage for each discharge - 3 joules
5. Gas mix - 20% CO_2, 10% N_2, 70% He
6. End reflector (copper) - 5-meter radius of curvature
7. Output flat (ZnSe) -
   Designator - 80% R
   Cross-wind sensor - 90% R
8. Mode-limiting aperture - .300" diam.

SECTION 3

CIRCUIT CONFIGURATION AND INITIAL EXPERIMENTS

Before beginning a discussion of the pulser circuitry chosen for the Incoherent TEA Laser units, it will be informative to briefly examine other circuits which were considered and describe some of the experiments which were performed with them. The circuits will be discussed in terms of the cross-wind sensor application, which requires two separate pulsers. The designator requirements are generally the same except that only one pulser, with the same total stored energy, is required.

Perhaps the simplest configuration for providing the required pulsed electrical conditions is shown in Figure 3. This circuit provides a useful background for discussing many of the difficulties which are commonly encountered in this type of work. The most severe problem is that the power supply must be capable of producing 24 kV output from 28 V input. As far as we know, there is no manufacturer capable of producing a small modular supply which will perform reliably at this voltage level. Also, the circuit of Figure 3 produces voltages of 24 kV with respect to ground and the problem of corona or arc breakdown to the grounded enclosure exists. The energy storage capacitors and the switches must both be capable of withstanding a charge voltage equal to the full pulsed requirement. The high voltage diodes, which isclate the two halves of the circuit during the discharge cycle, must be capable of surviving 24 kV transients. One final problem is that, without logic control of the charging cycle, the circuit of Figure 3 allows a keep-alive-type current to flow through the switch as recharging begins and the switch is reverting to a nonconducting mode. This forces the gap into a temporary, highly dissipative mode which shortens gap life. Ultimately, the gap fails by "hanging up" or conducting throughout the charge cycle, preventing the capacitors from reaching full charge.

Initial experiments were conducted with the circuit of Figure 3 using special versions of the GP-46B spark gap manufactured by EG&G. The value of C was .065 μF and the charge voltage was 17.5 kV. The GP-46-type gaps would not hold off the

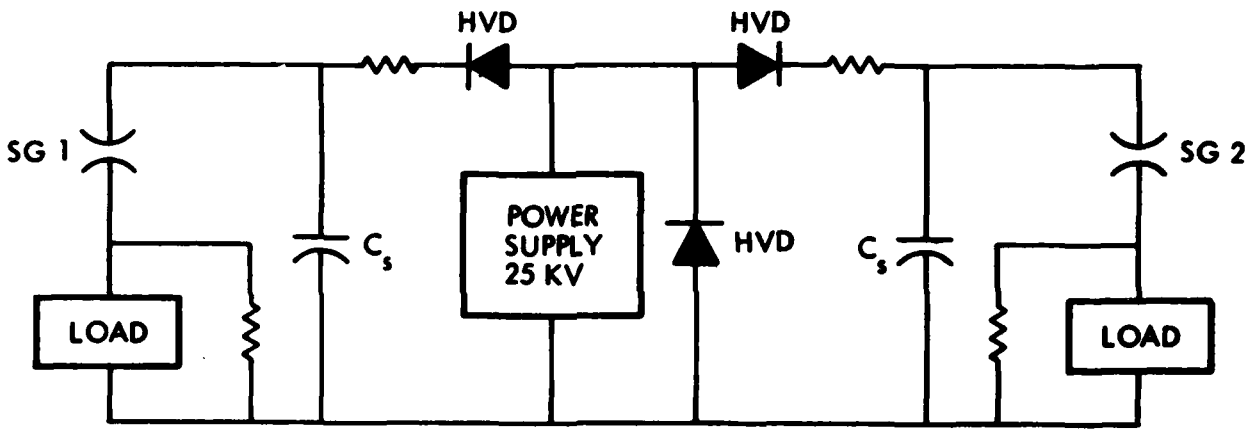

HVD - HIGH VOLTAGE DIODE
SG1,2 - SPARK GAPS
C_s - ENERGY STORAGE CAPACITORS

EOA-2647

Figure 3. 25 kV Double Capacitive Discharge Circuit

charge voltage after a few thousand shots. One of the gaps, which operated for about 8,000 shots before it failed completely, was broken open and found to have a fairly large amount of sputtered material on the walls. It appeared that this sputtering was the cause of the gap's inability to hold off the charge voltage.

Further tests were conducted with standard GP-70 gap. With proper triggering, these gaps survived for more than 400,000 shots before failing. The tests subjected the gaps to peak switching currents of approximately 5,000 amps, with stored energies of more than 10 joules switched to the load. The ultimate failure mode of these gaps was not the inability to hold off the charge voltage, but instead it was that the gaps continued to conduct during the recharge cycle. It was felt that this was not really a problem with the gap, but rather a problem with the charging circuitry. The use of logic-controlled charging supplies which could be disabled during the firing of the gap would eliminate this problem.

Another important point to note is that long life of the spark gap can only be achieved with proper triggering, especially when the load is another gas discharge device, such as a TEA laser. The normal mode of conduction through a spark gap is by means of a constricted high current density arc. The arc is fed by metal ions supplied by a hot spot on the electrode of the switch. The constricted arc has very low impedance, with the result that small quantities of energy are deposited in the switch. Low energy dissipation is essential for long switch lifetime. During the discharge initiation phase of the circuit of Figure 3, a spark gap should properly be allowed to make a rapid transition to a high current arc. However, the laser discharge current cannot build up as rapidly as one might like, since the discharge is inductive during its formative phase. Thus, the spark gap operates for a period of time in a current starved, highly dissipative mode - a mode which shortens the life of the gap. This is an important problem which exists for all circuits using a spark gap to switch energy to a gas discharge load. There are two possible solutions to this problem.

One involves placing a small capacitor (500 pF) directly in parallel with the spark gap. When the gap is triggered, it immediately makes the transition to a high-current constricted arc by discharging the parallel capacitor. The low inductance of this parallel combination prevents ringing. This occurs no matter what the characteristics of the remaining circuit may be. The finite time required to discharge the capacitor keeps the spark gap in a low loss mode until the main laser discharge has had time to form. Once this occurs, the spark gap switches the remaining stored energy efficiently, even though the laser discharge may limit the spark gap current to a few kA. After this has been accomplished, the gap can revert to a lower current level without becoming dissipative.

Another solution to the problem of rapidly establishing low impedance in the switch is to apply a trigger pulse of such a high amplitude and of the proper polarity that the trigger pulse can break down across the gap. If there is sufficient energy in the trigger pulse, the gap will quickly drop to a low impedance state and remain in such a state until the laser discharge forms.

The spark gap experiments discussed previously led to the design of the triggering circuitry and choice of a spark gap switch for the Incoherent TEA Laser pulsers. The triggering circuitry provides 25 kV pulses with roughly 50 millijoules of energy. This has been shown to provide prompt, reliable triggering for several million shots. The spark gap chosen was the GP-70, filled for 35 kV static breakdown.

Figure 4 shows the details of an L-C inversion generator circuit which has been utilized to energize TEA laser loads in a number of applications. Ideally, this circuit produces voltage inversion across the capacitor in parallel with the spark gap, thus providing a voltage to the load of twice the charge voltage. In this ideal case, components with only one-half the normal voltage ratings are required. In practice, however, the inversion is never complete and a large fraction of the stored energy is dissipated in the spark gap. High peak currents and voltage reversal place unnecessary stress on the high voltage components of this circuit. In previous work with this circuit, Raytheon tested

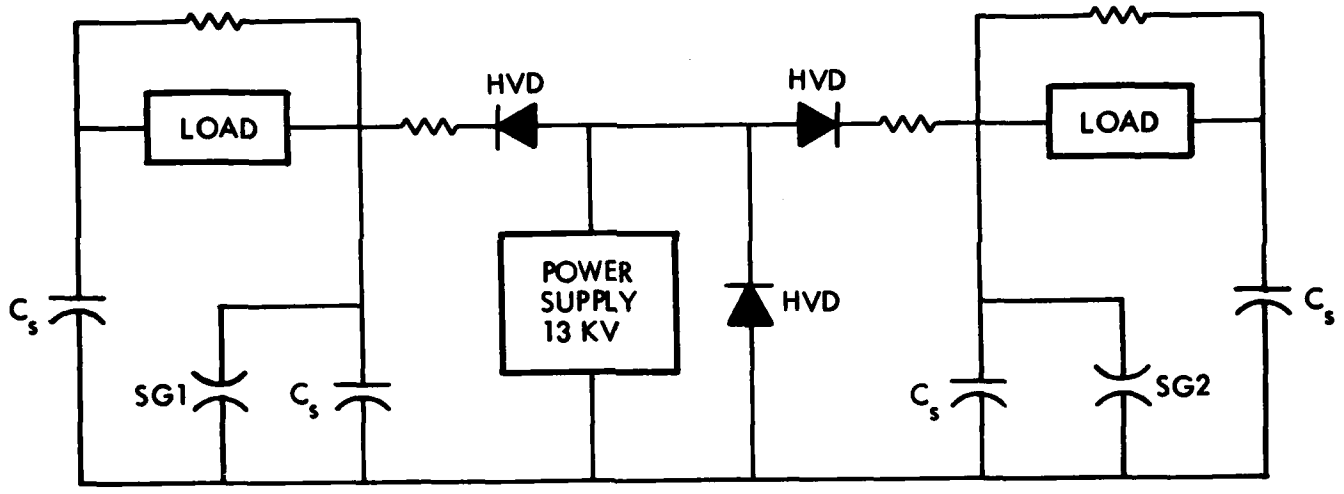

HVD - HIGH VOLTAGE DIODE

C_s - ENERGY STORAGE CAPACITOR

SG1,2 - SPARK GAP SWITCHES

EOA-2648

Figure 4. Double-Sided L-C Inversion Generator

a total of six GP-70 gaps. None of the gaps performed reliably after 50,000 shots and some failed after only 20,000 shots. Capacitor failure was also a serious problem.

A more effective voltage-doubling circuit, a 2-stage Marx unit, is shown in Figure 5. The capacitors are charged in parallel and discharged through the laser load in series. Triggering of the first gap doubles the voltage across the over-voltage gap in the second stage, which is designed to break down quickly under these conditions. With a 12 kV charging supply, storage capacitors, and switches, the required 24 kV can be provided to the load. This circuit was used successfully in some tests, but inability to accurately control the timing of the breakdown of the second gap is a severe limitation in cross-wind sensing applications. Also, the characterisitics of the over-voltage gap changed quickly, resulting in a short useful life.

As was mentioned earlier, the L-C inversion generator used to energize TEA lasers is very inefficient at delivering stored energy to the load. For example, in previous work with a designator laser similar to the one shown in Figure 1, more than 12 joules were stored in a pulser in order to produce a laser pulse with 125 millijoules energy. The cause of the low efficiency was the fact that most of the stored energy is dissipated in circuit elements other than the discharge load, thus leading to low efficiency and short lifetime of the other elements, such as the spark gap.

The circuit of Figure 6 avoids many of the problems discussed above, but still provides voltage doubling and allows the use of components rated at half the voltage which would otherwise be required. Operation of this circuit is described as follows: the two power supplies, plus and minus 10-15 kV with respect to ground, charge up the energy storage capacitors. A separate bias resistor in parallel with the load keeps any voltage from appearing across the load during the charge cycle. When the switch fires, the series combination of capacitors (20-30 kV) is connected across the load and energy is efficiently transferred from the capacitors to the load.

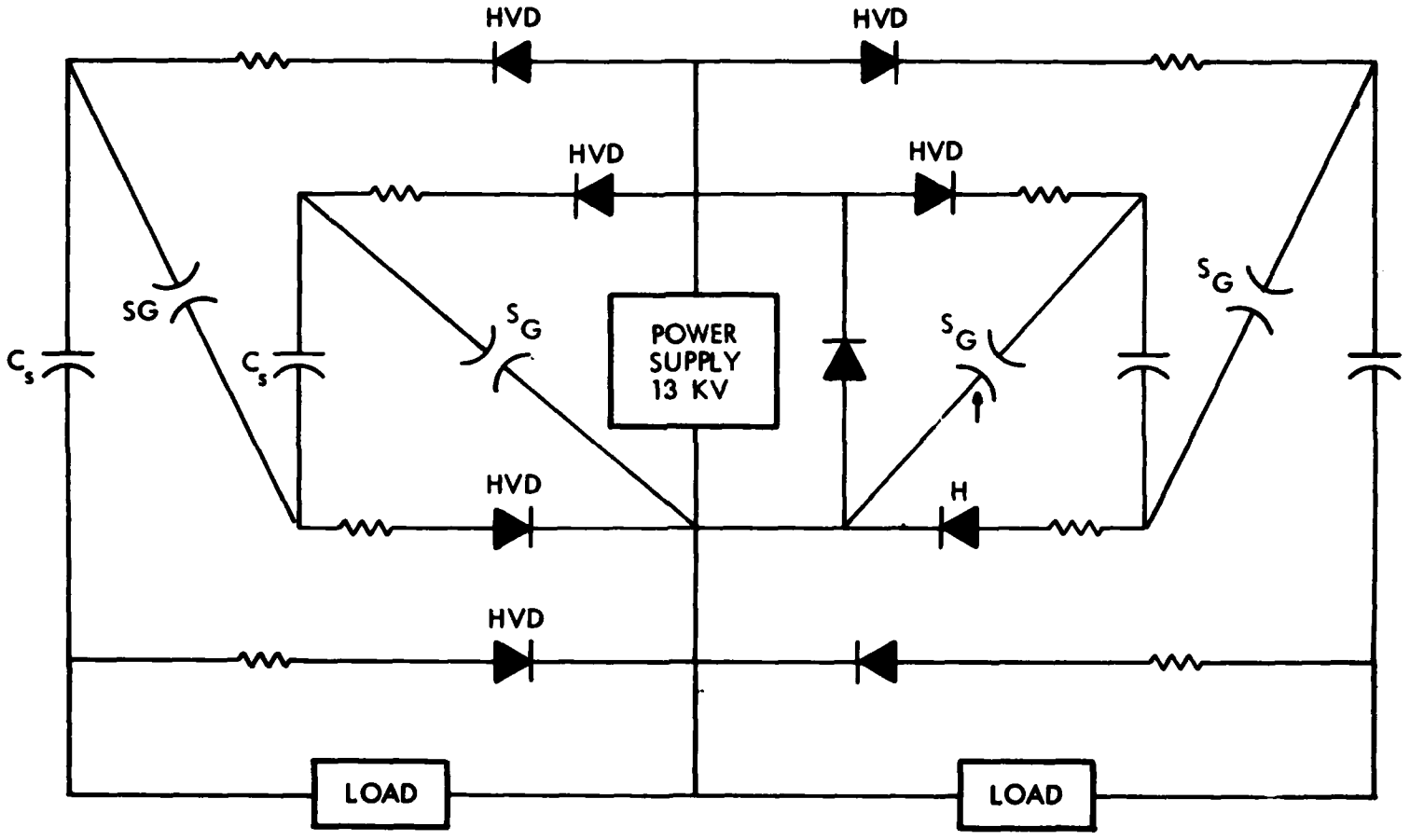

Figure 5. Double-Sided Two-Stage Marx Generator

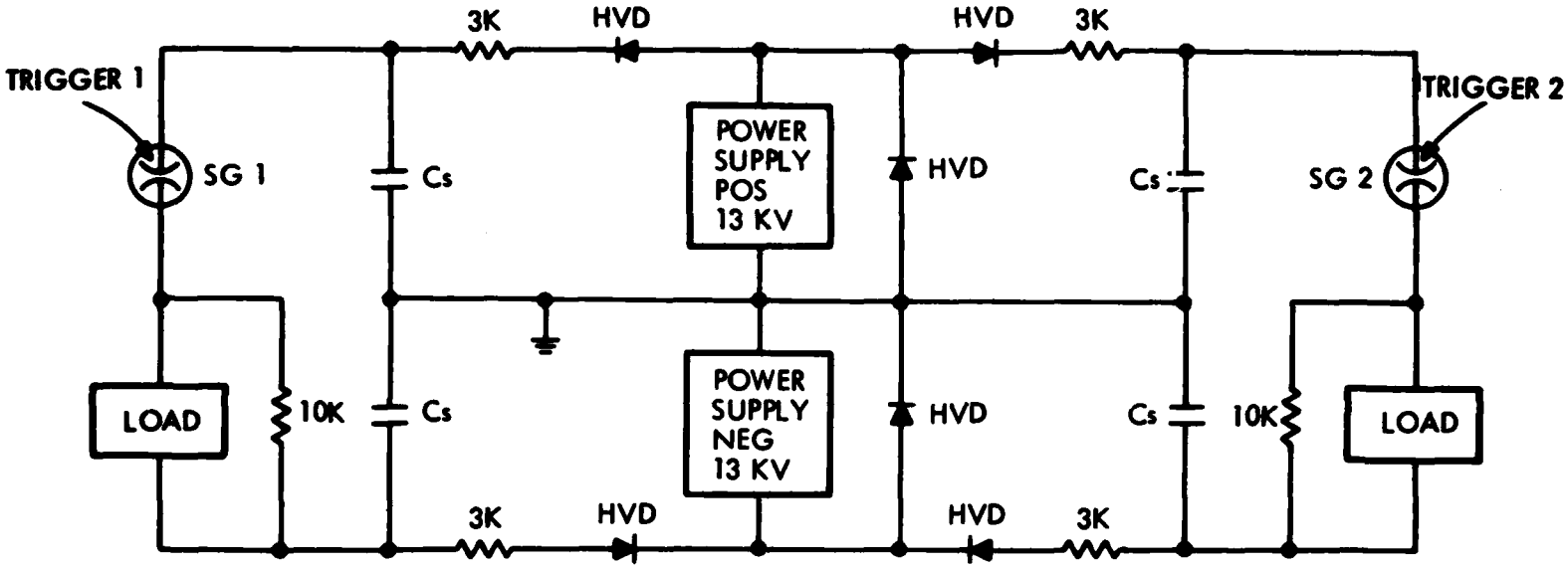

HVD - HIGH ENERGY DIODE

Cs - ENERGY STORAGE CAPACITOR - .02 μF

SG 1,2 - GP-70 SPARK GAPS

EOA-2650

Figure 6. Double-Sided Plus-Minus Charge Circuitry

There are several advantages to this type of voltage-doubling circuit. First, only voltages of 10-15 kV with respect to ground exist in this circuit, thus decreasing the chances for corona or arc breakdown to the grounded enclosure. The capacitors and the charging supply need to be rated at only half the required voltage to the load. Only the switch sees the full voltage. The circuit provides for nearly complete voltage doubling and efficient energy transfer to the load. The coulomb loading of the switch is minimized and the lifetime of the switch is thus maximized. Because of the simple components required and the convenience of packaging, the circuit of Figure 6 was used in fabricating the Incoherent TEA Laser pulsers.

The improved efficiency of the plus-minus charge circuitry of Figure 6 over the L-C inversion generator of Figure 4 becomes apparent when the two circuits are used to drive laser discharge loads. For a designator laser of the type shown in Figure 1, the L-C inversion generator stored 12.5 joules to deliver 125 millijoules in the laser pulse. The plus-minus charge circuit stored only 5.75 joules to deliver more than 200 millijoules from the laser. The decreased energy requirements which are brought about by the L-C inversion generator approach result in a significant reduction in the size of the energy storage capacitors and charging supplies. Table 1 shows a plot of laser output energy as a function of stored energy in the plus-minus circuit.

TABLE 1

LASER OUTPUT FOR VARIOUS VALUES
OF CHARGE VOLTAGE AND STORED ENERGY:
PLUS-MINUS CHARGE CIRCUIT

CHARGE VOLTAGE	STORED ENERGY	LASER OUTPUT
10 kV	4 J	160 mJ
11 kV	4.8 J	175 mJ
12 kV	5.7 J	200 mJ
13 kV	6.7 J	225 mJ
14 kV	7.8 J	250 mJ
15 kV	9 J	225 mJ

SECTION 4

ELECTRICAL COMPONENT SELECTION

4.1 ENERGY STORAGE CAPACITORS

The energy storage capacitors chosen for the Incoherent TEA Laser pulsers were mica paper or "reconstituted" mica. These capacitors can be fabricated in almost any shape with great flexibility of terminal configuration. Capacitance does not change greatly with age or charge voltage.

The capacitors used are of a special design, manufactured for Raytheon by Tobe Deutschmann Labs of Canton, MA. Each unit has four .02 microfarad capacitors rated at 25 kV. The electrical leads from the capacitive windings are copper flags contacted over a large area at the ends of the winding. The large surface area of the leads makes a low inductance contact capable of passing very high currents without being damaged. The internal leads of the capacitors are attached to 8-32 female inserts, which provide a convenient method of making external electrical connections and a sturdy mechanical attachment for mounting. The capacitors are designed for 25 kV even though only 12-15 kV will be placed on each capacitor. This margin of safety is required in order to ensure that the capacitors will survive at least 10 million charge-discharge cycles. An outline drawing of the capacitor is shown in Figure 7.

4.2 HIGH VOLTAGE BLOCKING CAPACITORS

High voltage blocking capacitors are required on the secondary side of the trigger transformer and in the preionizer circuitry of the laser. These capacitors are exposed to higher voltages (up to 30 kV) than the energy storage capacitors, but they pass very low peak currents. Also, the capacitance value of the blocking capacitors is quite low (500 pF) compared to the storage capacitors. For these reasons, it was felt that standard "doorknob" capacitors, with barium titanate

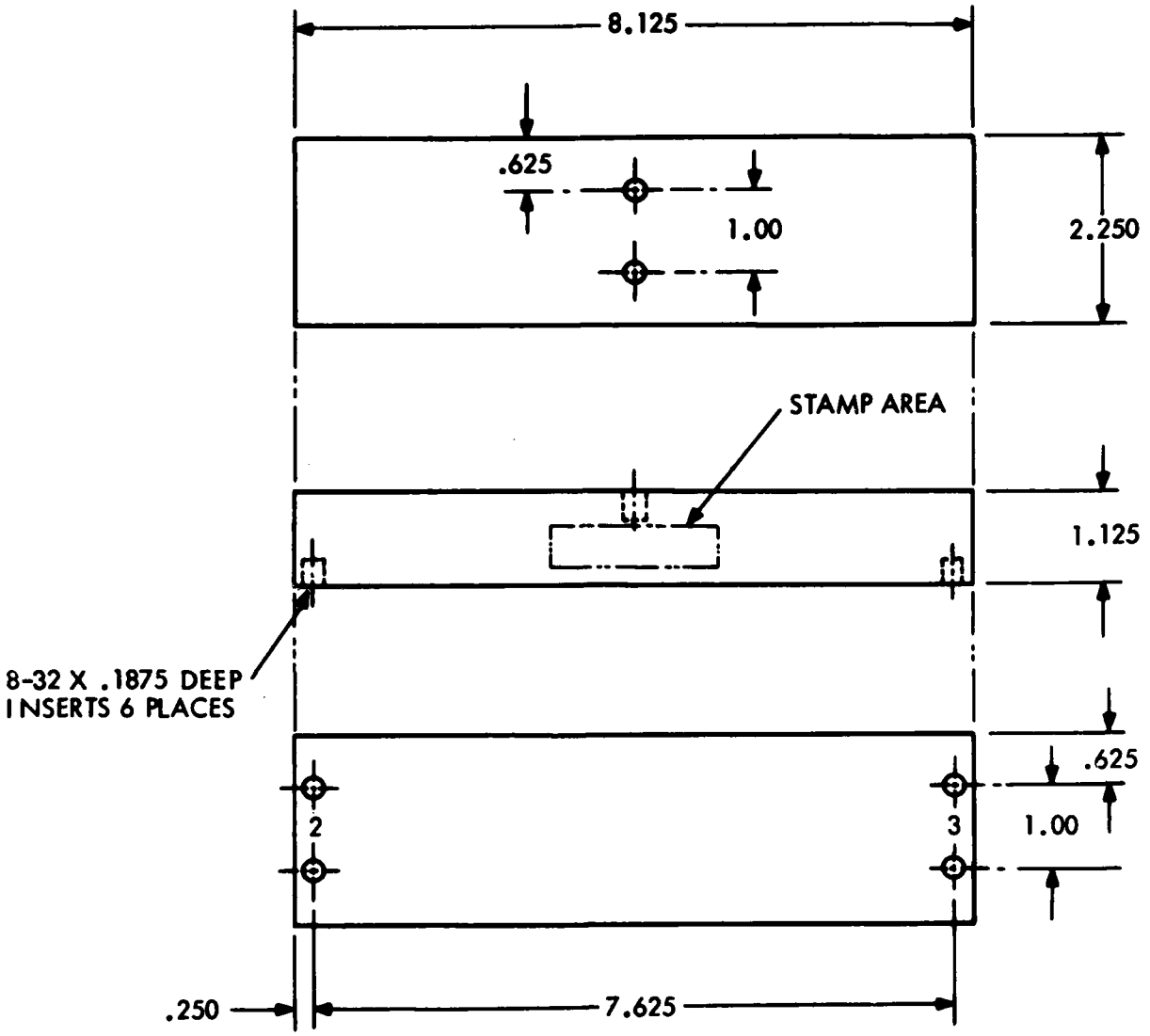

Figure 7. Energy Storage Capacitors

dielectric, would provide adequate electrical performance. The capacitors used in the pulsers were 480 pF, rated at 40 kV in order to assure long life. The manufacturer was Murata Corporation.

4.3 TRIGGER TRANSFORMERS

As was stated earlier, one of the requirements for long spark gap life is the use of proper triggering techniques. For the GP-70 spark gaps, it has been found that trigger pulses of only 10 kV will produce breakdown of a new gap, but as the gap ages, higher voltages are required. We have achieved best gap performance with trigger voltages in excess of 30 kV.

The trigger transformer used in the Incoherent TEA Laser pulsers is the U.S. Scientific Instruments Model #TT-180-42. A data sheet for this transformer is shown in Figure 8. The primary voltage level is set at 275 volts, and the primary capacitor is 1.5 μF. According to the data sheet, this gives a pulsed voltage to the gap of 30 kV. In actual practice, the voltage pulse is only 20 kV. This is caused by the use of a 2Ω resistor in the primary circuitry to limit the current going through the SCR. This resistor also cuts down the secondary voltage. Reliable triggering has been achieved for more than 3 million pulses; but at this point, the required trigger voltage on one of the gaps tested had risen to 18 kV. This led to failure to trigger the gap on roughly one shot out of 100. It is believed the reduction of the resistance in the primary circuit would extend the useful life of the system considerably.

4.4 SPARK GAP SWITCHES

Selection and testing of spark gap switches was carried out by Raytheon with assistance from the spark gap manufacturer, EG&G. Most testing was carried out early in the program under charge and energy transfer conditions which were more severe than the actual requirements to be encountered in the final units.

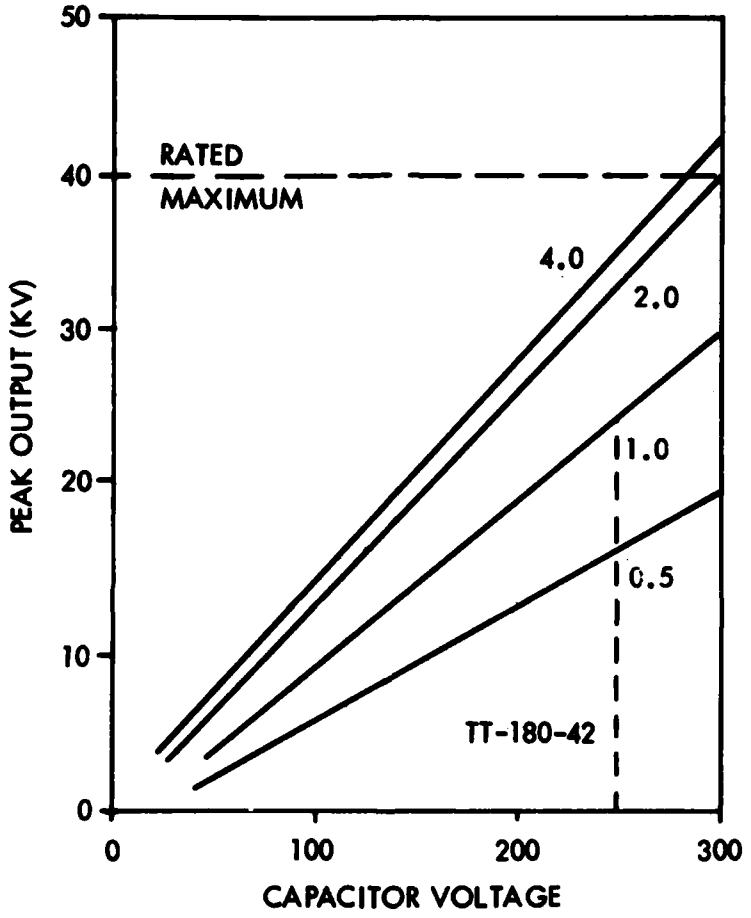

NOTE: FIGURES AGAINST CURVES REPRESENT VALUES OF CAPACITOR IN MICROFARADS

EOA-2652

Figure 8. Trigger Transformer Data

Two different types of gaps were studied: standard GP-70 gaps and various modified versions of the GP-46 gap. The studies with GP-46-type gaps were done with advanced electrode materials, including pure tungsten and an alloy of copper and tungsten. Also, gaps with a recessed trigger electrode were studied.

Experiments were carried out using a single-sided version of the capacitor discharge circuit shown in Figure 3. The value of the energy storage capacitor was .065 microfarads and the charge voltage was 17.5 kV, giving a stored charge of 1.25 millicoulombs and a stored energy of roughly 10 joules. The tests were conducted before it became apparent that proper circuit design could decrease energy-switching requirements by more than a factor of two. Also, the tests were performed before logic-controlled power supplies were available. In the case of the GP-70 gaps which were tested, this led to a failure mechanism which was caused by the charging supplies and not gaps themselves.

All the GP-46 body gaps which were tested failed with very few shots, while the unmodified GP-70 gaps survived for a much longer time. As a result of these tests, the final pulser configuration was designed to accommodate GP-70 gaps. From these preliminary tests, it was clear that the GP-70 gaps would provide a greater safety margin in the pulser design and it was felt that this additional margin would be necessary in achieving overall system lifetime of several million shots.

4.5 HIGH VOLTAGE CHARGING SUPPLIES

From the preceding discussion, it is apparent that the high voltage charging supplies are an important factor in determining overall system performance and lifetime. The power supplies used in the pulsers are the Laser Drive Model #3015 P/N capacitor charging systems. Through an extensive engineering effort, Laser Drive has developed these units into reliable and efficient charging systems which are ideal for capacitor discharge applications. The units feature a combined energy storage and transfer scheme which utilizes the inductive impedance of the high voltage transformer to eliminate the need for lossy series charging

resistors which are normally required in capacitor charging applications. The units are compact, but advanced construction and encapsulation techniques allow corona-free operation of the high voltage stages assuring long life. The units have versatile control and gating functions which allow internal or remote programming of output parameters. Energy transfer rates of 100 joules per second are possible with conversion efficiencies approaching 90%. Detailed information on the packaging, the internal electronics, and the requirements of the supplies is contained in the appendix with the discussion of the control electronics. Aside from mechanical problems encountered early in the development effort, the units have performed without failure for millions of charging cycles.

SECTION 5

OPERATIONAL TESTS OF ELECTRICAL CIRCUITRY

One of the completely assembled electrical pulsers is shown in Figure 9, and the same unit is shown with a laser inserted in Figure 10. The high voltage circuitry with the two laser discharges and their associated preionizers are shown in Figure 11. Triggering circuitry for the spark gaps is shown in Figure 12, and the details of the control logic circuity are discussed in the appendix.

The operation of the circuit has been described previously, but will be repeated here with more detail. Activation of the high voltage section of the pulser is initiated when a reset pulse from the logic section is applied to the charging supplies. This pulse enables both the positive and negative supplies. The upper capacitors in each half of the circuit are charged positive with respect to ground and the lower capacitors are charged negative with respect to ground. Charging waveforms for the positive and negative supplies are shown on two different time scales in Figure 13, and the complete charge and discharge cycles of the capacitors are shown in Figure 14. Note that the 3 kΩ resistors in series with each of the four energy storage capacitors during the charge cycle do not limit the charging current. The charging currents are controlled by the internal electronics of the supplies. The sole function of the series resistors is for protection of the supplies from voltage transients which might occur if a fault occurred in the discharge loop while the supplies were still enabled. Also, it should be pointed out that the series resistors dissipate less than 2% of the energy delivered by the supplies. Figure 13 shows that the maximum charging currents are roughly 20 mA, so that I^2R losses in the resistors are less than 1 watt during the charge cycles. Integrated losses during the 25-35 millisecond charge time are roughly 30 millijoules, whereas the total delivered to each capacitor is more than 2 joules. If the charging supplies had no internal control of current levels, it would be necessary to use resistive ballasting, and 50% of the energy delivered by the supplies would be lost in heating the resistors. This would necessitate the use of power supplies with twice the power capabilities of those now being used.

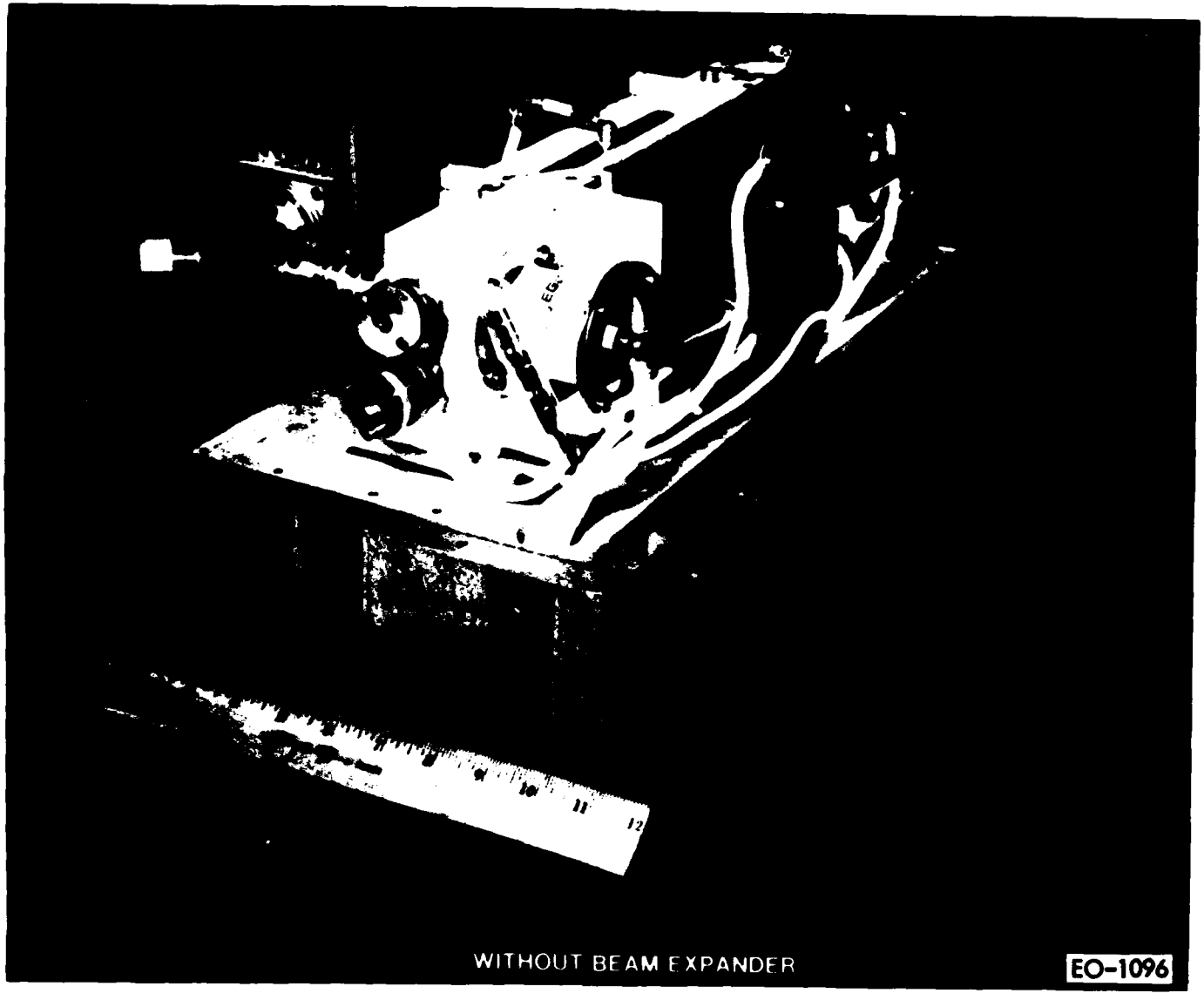

Figure 9. Pulser with Laser

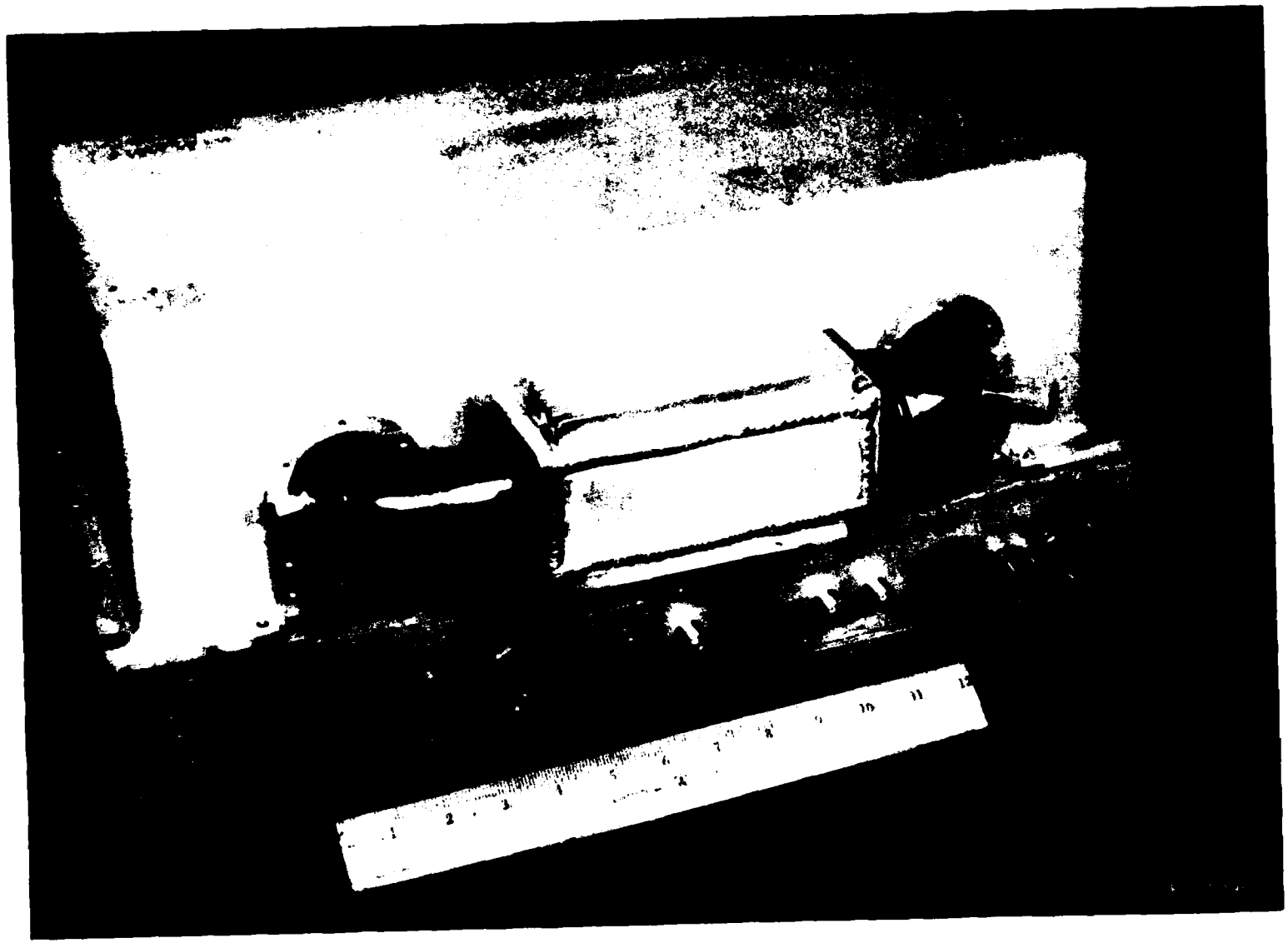

Figure 10. Complete Pulser with Laser

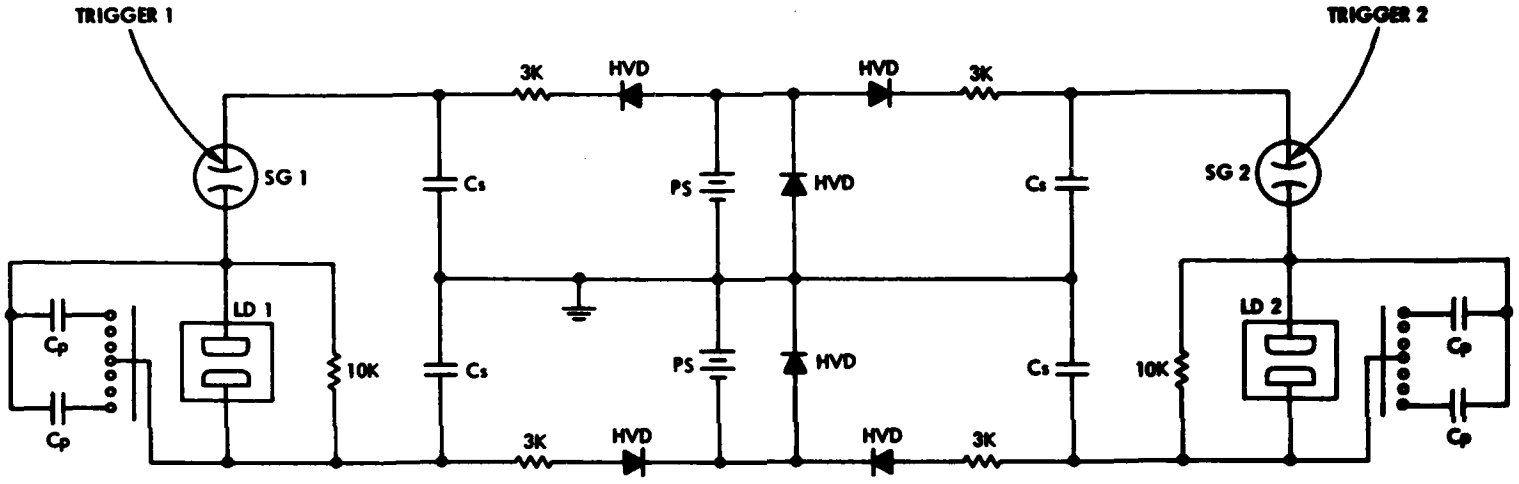

PS - HIGH VOLTAGE CHARGING SUPPLY - 100 WATTS, 20kV
HVD - HIGH VOLTAGE DIODE
Cs - ENERGY STORAGE CAPACITOR - .02 μF
SG 1,2 - GP-70 SPARK GAPS
LD 1,2 - LASER DISCHARGES
Cp - PREIONIZER CAPACITORS - 340pF

EOA-1949

Figure 11. Pulser Circuitry

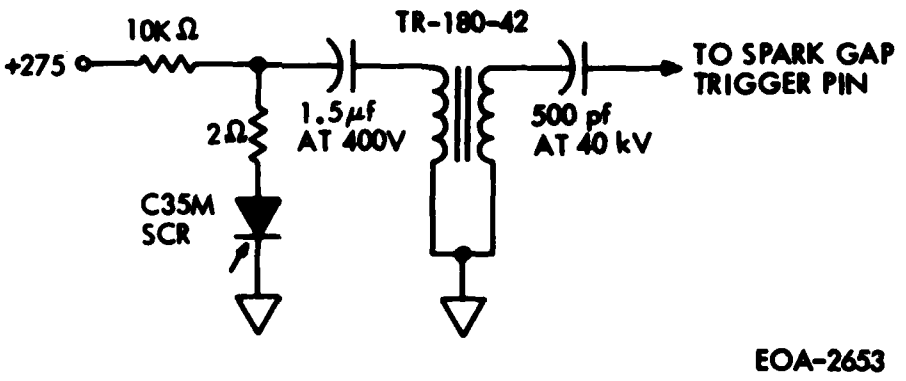

Figure 12. Spark Gap Trigger Circuit

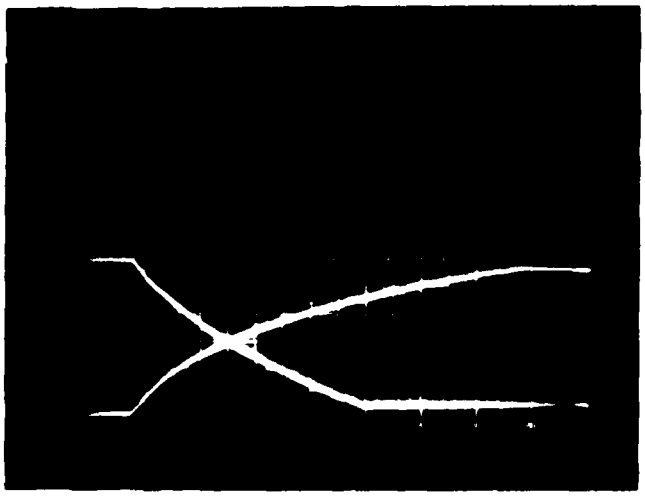

Charge Cycle of Positive and Negative Supplies

5 kV/Div.

5 ms/Div.

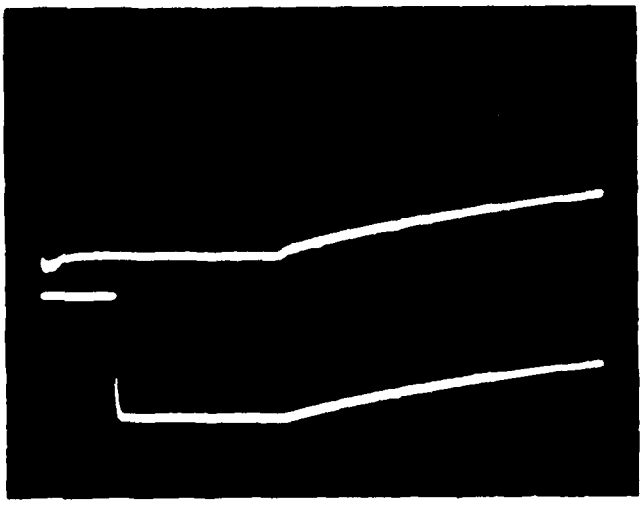

Firing and Recharge Cycle of Positive Supplies

Note Delay of Firing (1.4 ms) and Recharge (4.4 ms)

5 kV/Div.

1 ms/Div.

EO-1225

Figure 13. Charging Waveforms

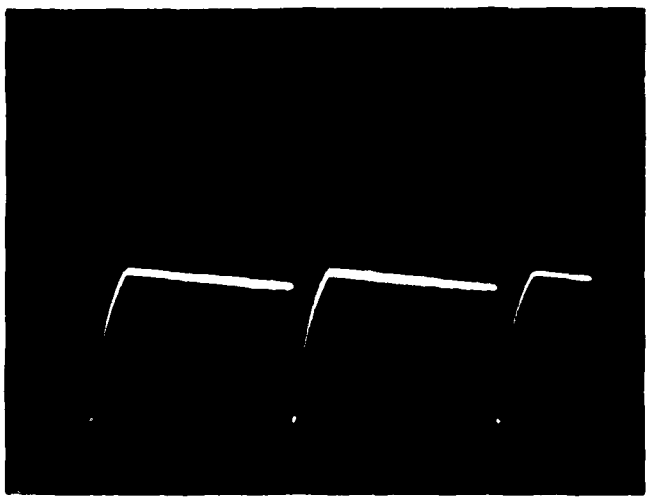

Positive Supply Charge-Discharge Cycle

5 kV/Div.

50 ms/Div.

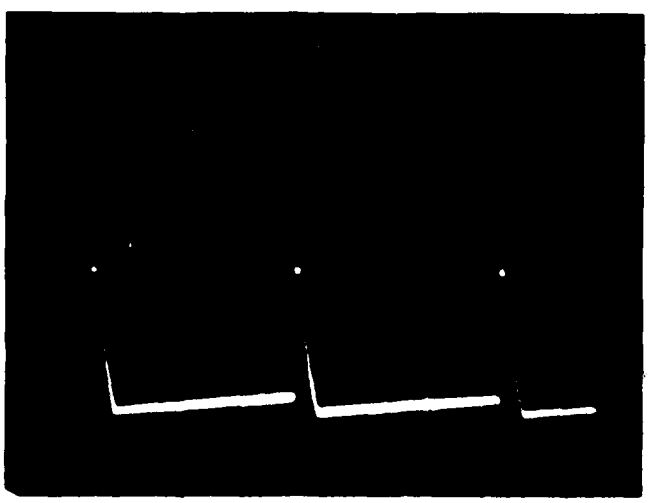

Negative Supply Charge-Discharge Cycle

5 kV/Div.

50 ms/Div.

NOTE: Voltage decay between pulses is caused by monitoring probe impedance

EO-1226

Figure 14. Charge-Discharge Cycle 5.5 Hz

The charge cycle is terminated when the capacitors are charged to a predetermined level. The internal voltage sense of each supply disables the power oscillator and causes the disable output to change voltage states. The disable outputs from the two supplies are fed back to the logic control circuitry. When the charging supplies are disabled, the logic pulsing circuitry is enabled; that is, logic pulses generated either externally or internally within the unit can be fed through to the gates of the SCR switches located in the circuitry on the primary side of the trigger transformer. Discharging the primary side capacitor generates a trigger pulse at the secondary of the transformer which is capacitively coupled to the trigger pin of the spark gap. Capacitive coupling of the trigger is necessary because the spark gap trigger pin is charged to high voltage and the transformer secondary is grounded. Figure 15 shows typical trigger pulses both into an open circuit and into a GP-70 spark gap. Note that the voltage available is nearly twice the required breakdown voltage. This gives reliable triggering for millions of shots.

With the firing of the spark gaps, the energy stored on the capacitors is transferred to the load. Typical voltage and current waveforms are shown in Figure 16. These are the waveforms which result from discharging the capacitors through a small value of resistance which gives an underdamped circuit. Examination of the waveforms reveals that the inductance of each discharge loop is roughly 1 microhenry. Part of this inductance is in the leads and the spark gap. Figure 17 shows the voltage waveform when the pulsers fire into a laser discharge load with characteristics identical to the lasers used in the Incoherent TEA Laser.

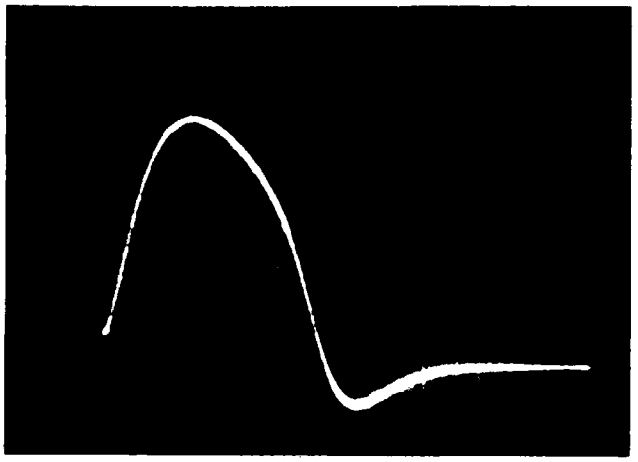

Open Circuit Trigger Voltage

5 kV/Div.

2 μs/Div.

Trigger Pulse to New GP-70

5 kV/Div.

2 μs/Div.

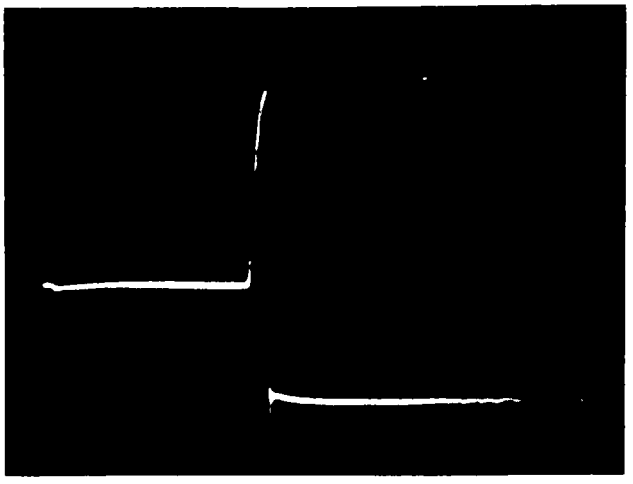

Trigger Pulse to GP-70 Gap with 3.2×10^6 Shots

5 kV/Div.

10 μs/Div.

EO-1227

Figure 15. Spark Gap Trigger Pulses

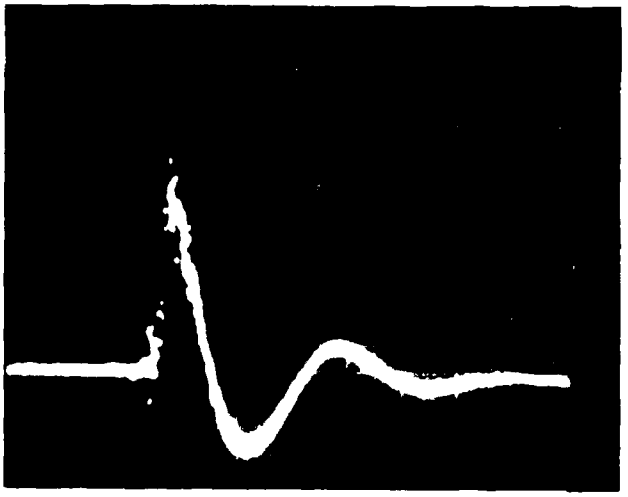

Load Voltage

5 kV/Div.

200 ns/Div.

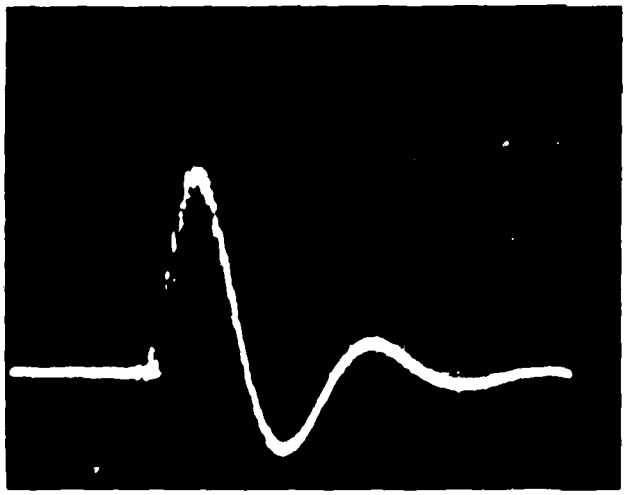

Load Current

400 A/Div.

200 ns/Div.

EO-1228

Figure 16. Pulser Voltage and Current Waveforms 2 Ω Load

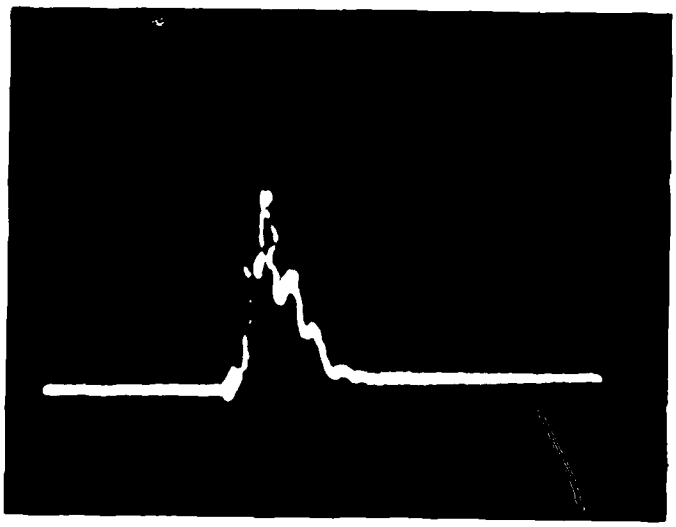

5 kV/Div.
200 ns/Div.

EO-1233

Figure 17. Voltage Across Laser Discharge

SECTION 6

LASER TESTS AND RESULTS

Three completely assembled pulsers capable of powering the cross-wind sensor and designator lasers were tested extensively as part of a separate program. These tests included firing the pulsers into resistive loads and laser discharge loads. The adequacy of the electrical design, from the standpoint of both component lifetime and production of the desired laser performance, was verified for these units.

As was mentioned earlier, initial experiments performed with a plexiglass laser and flowing gas led to the choice of many of the design parameters for the final alumina body lasers. Tests with the alumina lasers revealed that their performance was not as good as anticipated, partly due to inaccuracies in the machining of the laser bodies. The alumina body lasers produced 125 millijoules output, whereas the plexiglass laser of the same form produced over 250 millijoules when used with the same pulser.

Interferograms of the optical elements showed that the individual elements were good. Figure 18 shows interferograms taken to characterize the optics of the units.

Unit B was operated with removable flashboard covers and flowing gas. The performance which was achieved was approximately 50 millijoules in each pulse. The unit was operated at rates up to 5 hertz for short periods of time with no flow loop, and the energy output did not decrease significantly, although shot-to-shot reproducibility was degraded.

Unit B was operated sealed at 5 hertz for a total of 250,000 shots, at which time the output energy was only 5 to 10 millijoules in each of the two pulses. The shot-to-shot repeatability was poor, with many missing pulses.

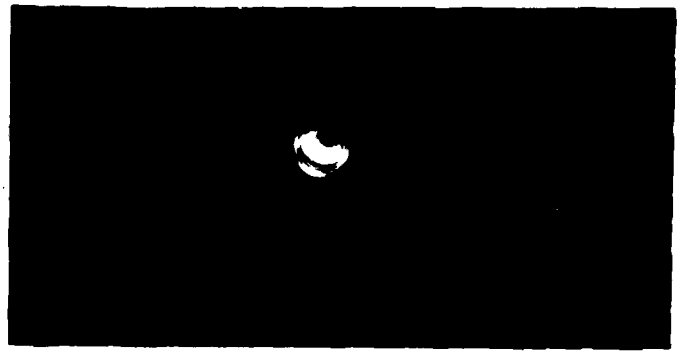

Output Coupler

Flatness better than 1/2 Wave in Visible

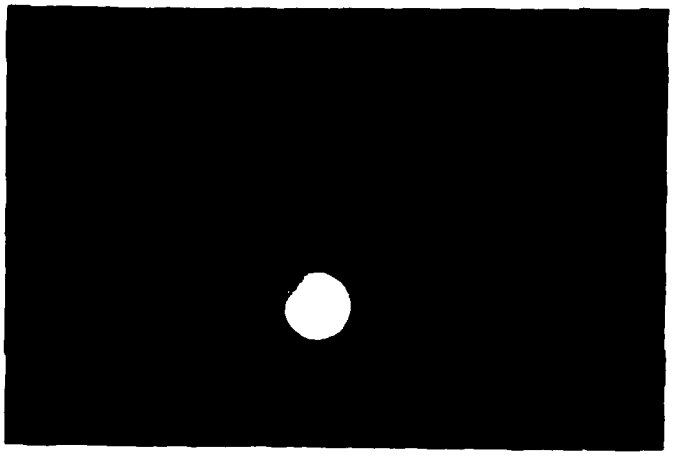

Curved Total Reflector

5-m radius

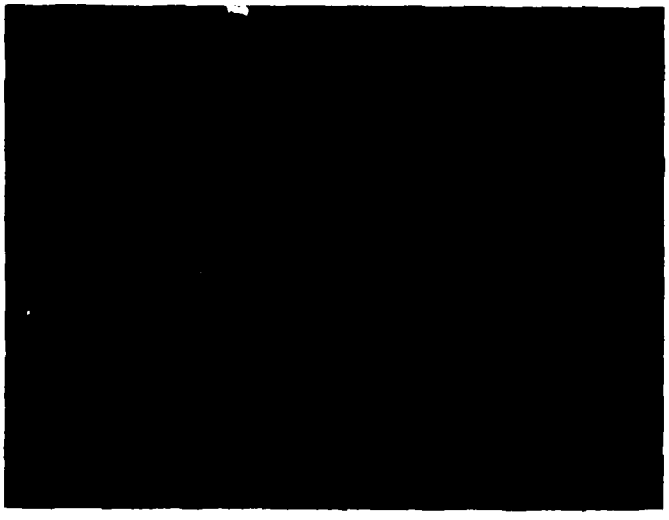

Interference Pattern of Curved Total Reflector and Turnaround Flats Mounted on Laser

EO-1229

Figure 18. Interferograms of Optical Components

The mirrors were removed and examined, and it was found that the copper turnaround mirrors were badly damaged, with less damage to the output coupler and the curved copper reflector which were located at the other end of the laser. Since the flow through the laser was directed at the damaged turnaround mirrors and away from the less severely damaged mirrors at the other end, it seemed likely that solid debris carried by the flowing gas was responsible for the damage. Analysis of the mirror surface showed very little surface contamination, with the main problem being physical abrasion of the mirror surfaces. SEM analysis of the mirror surfaces showed no foreign material other than a very small amount of cobalt. The damage to the mirrors was due to physical abrasion, not the deposition of foreign particles.

The double-pulse performance of the laser is shown in Figure 19. Relative energy in the two pulses can be varied by realigning the output coupler. Figure 20 shows the result of firing one side of the laser alone. The repeatability from shot to shot is clearly not the same for the two discharges. Small changes in the alignment of the output coupler can change the relative repeatability of the two sides.

The temporal behavior of the optical pulse shown in Figure 21 is not significantly different for the two sides of the laser, regardless of the alignment or gas mix.

Figure 22 summarizes the performance with life. The two dominant problems associated with the laser were that the location of the discharge changed with time relative to the optical cavity and that the optical cavity itself was difficult to align.

The performance of Unit A, the target designator unit, was similar to Unit B. After an initial test period, during which the electrodes were aligned for best discharge appearance, the laser was assembled with epoxied flashboard covers. Output energy was initially 150 millijoules, but after a few thousand shots,

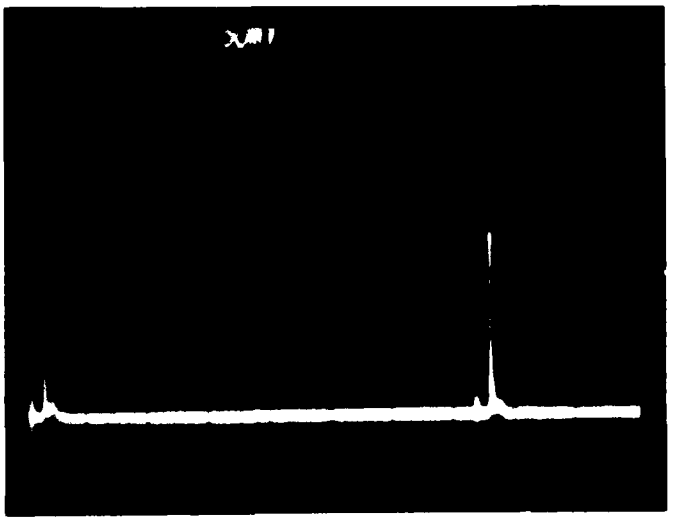

5 μs/Div.
17 mJ in each pulse
6 Hz rep rate

EO-1234

Figure 19. Sequential Output Pulsing of Cross-Wind Sensor Laser

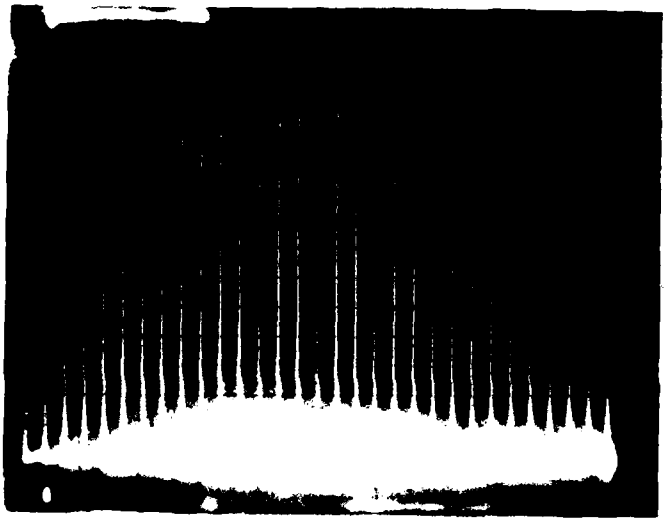

First Side
Pulsing Alone

1 Hz, 50 mV/Div.

~25 mJ/pulse

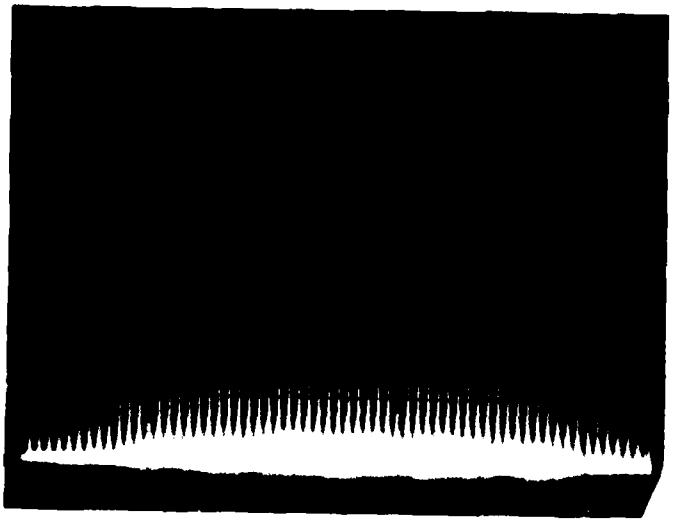

Second Side
Pulsing Alone

1 Hz, 50 mV/Div.

~11 mJ/pulse

EO-1230

Figure 20. Output Characteristics from Firing Each Discharge Alone

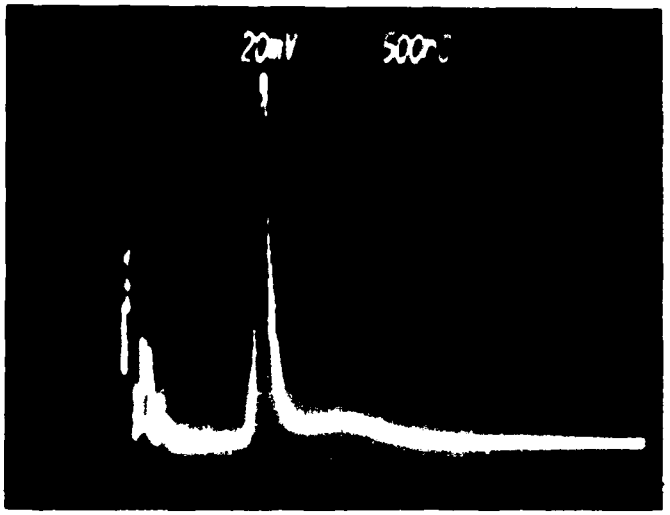

~ 13 mJ Output
500 ns/Div.

EO-1231

Figure 21. Output Pulse Shape

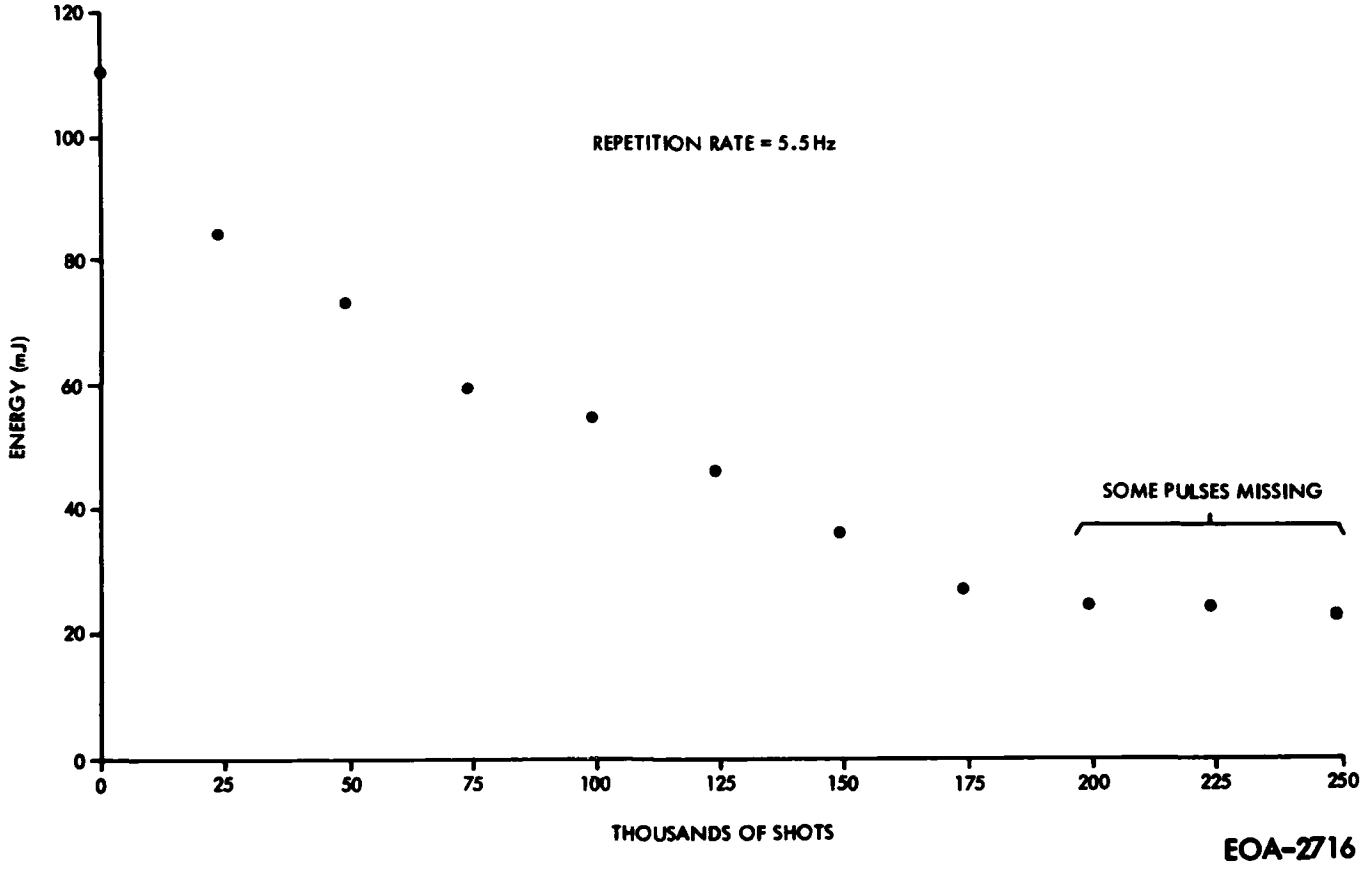

Figure 22. Laser Output vs Lifetime (Total Energy in Both Pulses of Cross-wind Unit)

the discharge had shifted away from the flashboard and the energy dropped to less than 100 millijoules. The laser was operated at high repetition rates for brief periods in order to determine the limits of the power supply and the cooling loop. Figure 23 shows the energy output as a function of repetition rate and Figure 24 shows the shot-to-shot reproducibility with flowing gas.

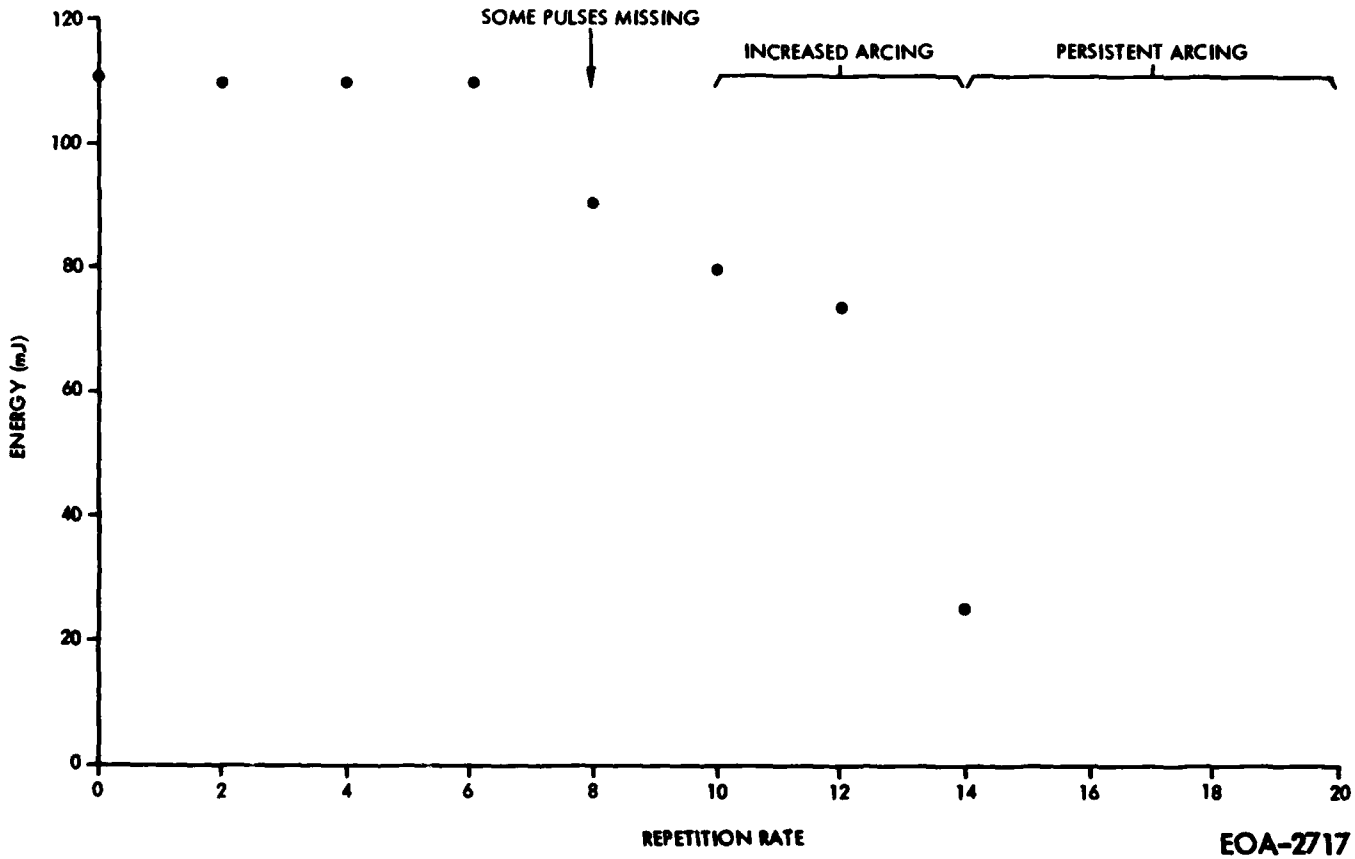

Figure 23. Laser Output as a Function of Repetition Rate (Designator Unit, Flowing Gas)

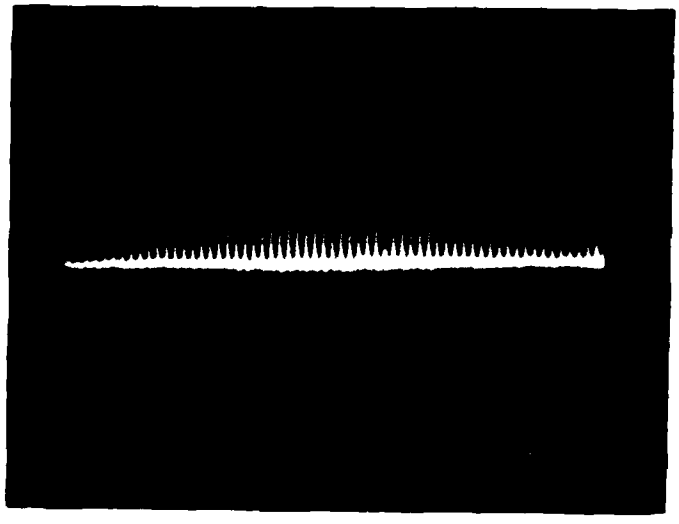

~100 mJ pulse
5.5 Hz

EO-1232

Figure 24. Shot-to-Shot Repeatability of Designator Laser with Flowing Gas

SECTION 7

SUMMARY AND CONCLUSIONS

The Incoherent TEA Lasers contract resulted in the design, fabrication and assembly of two CO_2 laser transmitter units. The lasers used in these units were fabricated from alumina ceramic. The original design of the lasers called for metalized seals, but a number of problems were encountered in pursuing this approach and epoxy seals were eventually employed.

Adequacy of the electrical design of the units was verified as part of a separate contract. The high voltage charging, energy storage, and firing functions of the units have been shown to produce the desired laser performance in a non-sealed laser. In addition, repetition rate and double-pulse functions have been suitably controlled in the high noise environment. Lifetime of all electrical components has been tested beyond 3×10^6 in work closely related to this contract. Problems have resulted in production of lasers with lower than anticipated output energy. A considerable amount of work remains to be done in the area of tube fabrication, especially with respect to seals of optical elements and alignment techniques. These techniques are currently being addressed under other programs.

APPENDIX A
CONTROL ELECTRONICS AND POWER SUPPLY LOGIC

The electronic control circuitry consists basically of four sections. Figure A-1 is a quasi-block diagram of these four sections.

Section 1 consists of the internal timer clock (U1-555 timer), the Auto/Manual mode switch, the laser fire switch and all combinational logic up to the Internal/External mode switch. The internal timer clock (U1) is always enabled (provided power is on). The Manual/Auto switch simply enables or disables the internal clock timer from continuing through the network. In the manual mode, the clock timer output is disabled and the laser fire switch (momentary) becomes operational, enabling one clock pulse to be generated for each depression of the fire button. The External/Internal switch makes it possible to provide an external clock. In the Internal mode, the external clock line is disabled (floating) and the internal clock (dictated by the Manual/Auto switch) is allowed to continue into Section 2.

Section 1 consists of the monostable multivibrator (one shot) U6 (Pins 10, 5) which feeds U20 Pin 1; U3 which feeds U20 Pin 2; a two-stage one-shot/delay network (U5,U6); and the 55114 Differential Line Driver (U19). On the rising edge of U6 Pin 10, U6 Pin 5 puts out a 10 μs pos. pulse. This pulse is only allowed to pass into the two-stage one-shot/delay network provided both the duty cycle (DC) and the laser ready (LR) are HI (Sections 3 and 4). When these enables are present, U5 Pin 2 is triggered by this 10 μs pulse which in turn triggers U5 Pin 10, causing U6 Pin 12 to put out a neg. pulse (pos. and neg. refer to Pos. Logic and Neg. Logic) that is of variable width. It is when this pulse expires that U6 Pin 2 is triggered, causing U6 Pin 13 to put out a pos. pulse. The signals on U5 Pin 4 and U6 Pin 13 are fed into the 55114 Line Driver. This dif-

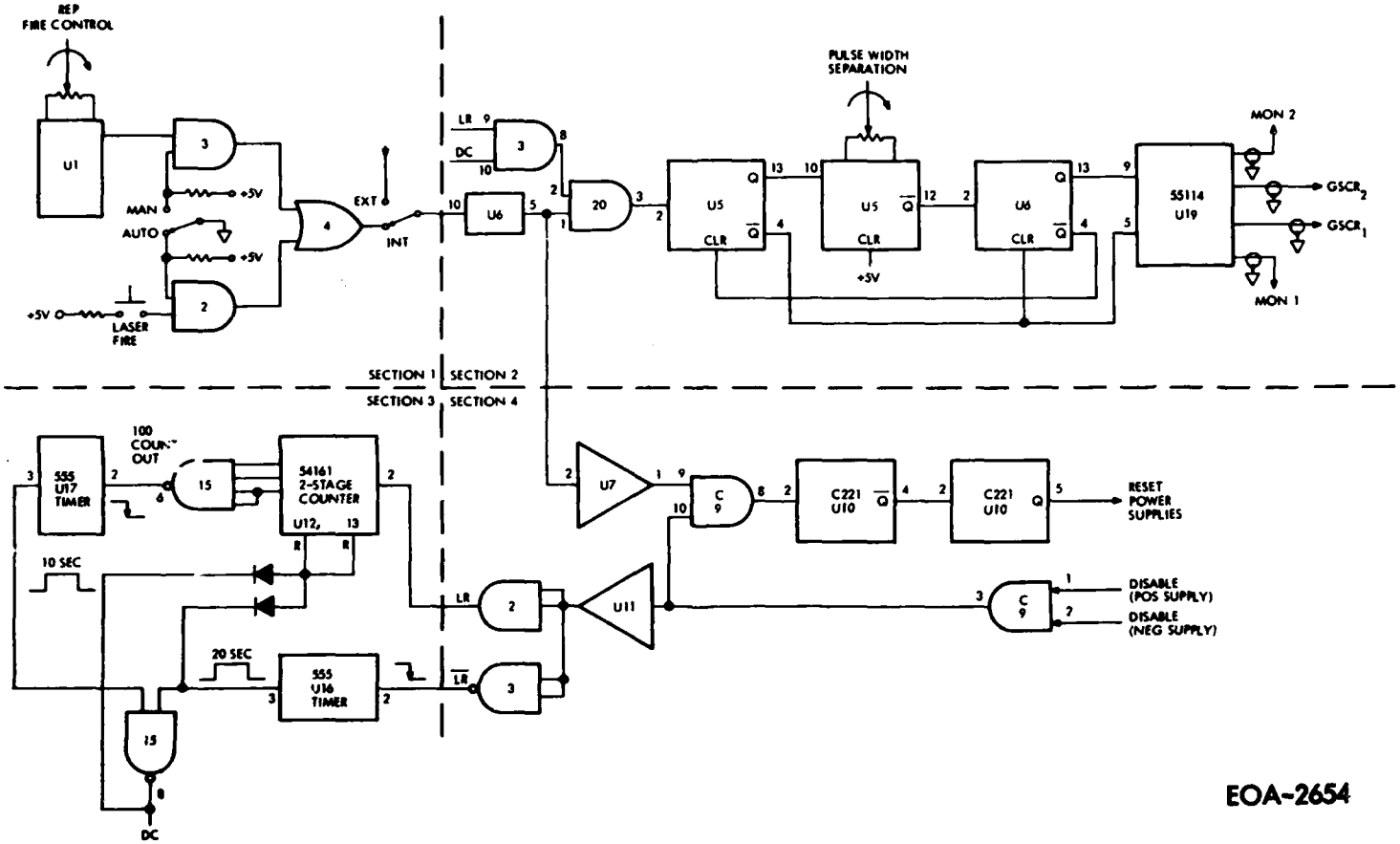

EOA-2654

Figure A-1. Dual Pulse Block Diagram

ferential line driver is being used in a single-ended fashion to drive the gates of SCR_1 and SCR_2 which in turn eventually trigger the two spark gaps. Due to the high noise environment, it becomes necessary to logically eliminate the possibility of uncontrolled pulsing, i.e., both spark gaps fire nearly simultaneously due to noise generated from the first gap firing. The solution to this problem involved connecting the $\overline{Q}$ (neg.) outputs of each of the two final one shots that fire the SCR's to the clear inputs of the other. This effectively eliminates the ability of both stages fire simultaneously. Neg. logic monitors are provided for the two SCR pulses.

Section 3 contains the hover-rep electronics. It consists of a two-stage (U12, U13) binary counter with two 555 times (U16, U17), as well as the interfacing combinational logic (U15). The two-stage counter is designed to generate a neg. edge when 100 LR pulses are generated, provided a counter reset pulse does not occur which will reset the counter to zero. Upon the first $\overline{LR}$ neg. edge (which corresponds to the first LR pos. edge), a 20-second pos. pulse is generated at U16 Pin 3. When this 20-second pulse falls, the counter is reset (through the diode) and a new 20-second pulse is generated when the next $\overline{LR}$ neg. edge occurs. It is essential to note that the 555 timer is NOT retriggerable, meaning that should $\overline{LR}$ edges occur while this 20-second pulse continues (and they do), they will not re-trigger the timer. Should 100 LR pulses be generated before the 20-second pulse falls, then a 10-second pos. pulse is generated at the output of U17. If this occurs, all inputs to U15 are HI and consequently U15 Pin 8 (DC) goes LO for 10 sec. (resetting the counter).*

---

*One firing of the laser may occur in this 10-second "shutdown" interval because the 20-second pulse may fall which would bring the Duty Cycle HI. This would allow one fire pulse to be generated. After this occurs, however, a $\overline{LR}$ neg. edge will start a new 20-second pulse which will shut down the system for the remainder of the 10-second interval.

Section 4 consists of a TTL-CMOS buffer stage (U7) which follows the one shot in Section 2 (U6 Pin 5). This buffered output is fed through U9 Pin 3 and is enabled to pass through U9 Pin 6 when BOTH DISABLE signals are present (HI) from the two Laser Drive Power supplies. This indicates the laser is ready (U3 provides the LR and $\overline{LR}$ functions in TTL levels). U11 provides the CMOS to TTL conversion.

Provided both disables are present from the power supplies and the 10 μs CMOS pulse is present on U9 Pin 6, a RESET pulse is generated at a fixed delay time from this 10 μs pulse. The operation of the Laser Drive Power Supplies is illustrated schematically in Figure A-2.

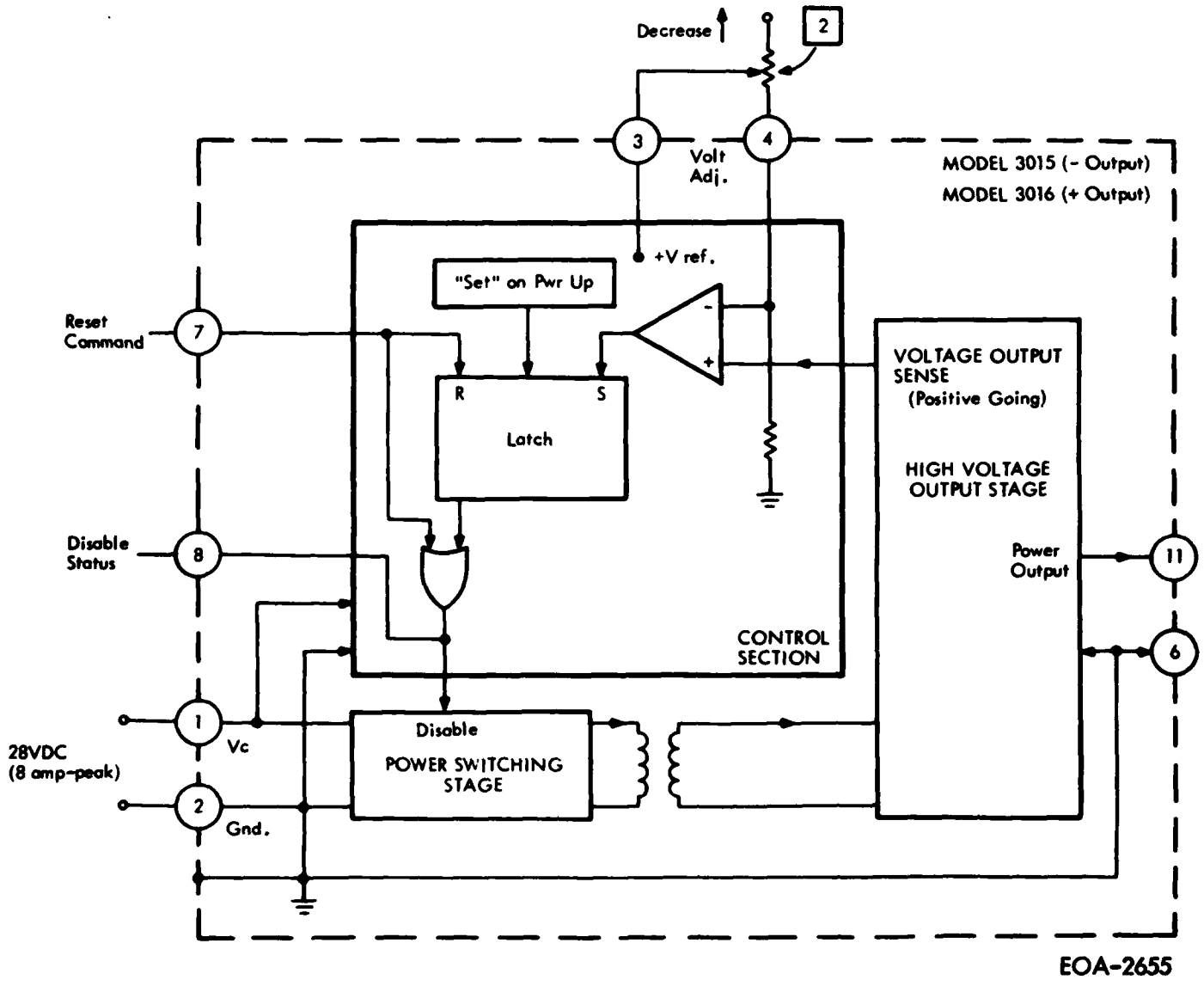

Figure A-2. High Voltage Power Supply

DISTRIBUTION LIST

	Number of Copies
Defense Documentation Center ATTN: DDC-TCA Cameron Station (Bldg 5) Alexandria, VA 22314	12
Commander U.S. Army Electronics Research and Development Command Night Vision and Electro-Optics Laboratory	
ATTN: DELNV-D	1
DELNV-L (Dr. R. Buser)	1
DELNV-L (Mr. Fox)	10
DELNV-SI (Mr. S. Gibson)	1
Fort Belvoir, VA 22060	
Commander U.S. Army Electronics Research and Development Command Atmospheric Sciences Laboratory ATTN: DELDS-AS-M (Mr. W. Vechione) White Sands Missile Range, N.M. 88002	2
Commander U.S. Army Electronics Research and Development Command Electronic Technology and Devices Laboratory ATTN: DELET-BG (Mr. M. Weiner) Fort Monmouth, N.J. 07703	1
Commander U.S. Army Armanents Research and Development Command Chemical Sciences Laboratory ATTN: DRDAR-CLC-CR (Dr. H. Walter) Aberdeen Proving Ground, MD 21010	1
Commander U.S. Army Missile Command ATTN: DRSMI-REO (Mr. L. Pratt) Redstone Arsenal, Alabama 35809	1
Project Manager, M60 Tanks ATTN: DRCPM-M60 (Mr. Ron McCullough) Warren, Michigan 48090	1
Project Manager XM-1 Tank System ATTN: DRCPM-GCM-SW (Mr. Lyle Wolcott) Warren, Michigan 48090	1

DISTRIBUTION LIST (Continued)

President 1
U.S. Army Armor and Engineer Board
ATTN: ATZK-AE-AR
Fort Knox, Kentucky 40121

Commander 1
U.S. Army Armor Center and Fort Knox
ATTN: ATZK-CD-TE
Fort Knox, Kentucky 40121

Director 1
Naval Research Laboratory
ATTN: Code 2627
Washington, DC 20375

Naval Surface Weapons Center 1
White Oak Laboratory
ATTN: Library, Code WX-21
Silver Spring, MD 20910

Rome Air Development Center 1
ATTN: Documents Library (TILD)
Griffiss AFB, NY 13441

HQDA (DAMA-ARP) (Dr. Verderame) 1
Washington, D.C. 20310

Cdr, US Army Avionics Lab 1
AVRADCOM
ATTN: DAVAA-D
Ft. Monmouth, NJ 07703

Cdr, US Army Research Office 1
ATTN: DRXRO-PH (Dr. Lontz)
P.O. Box 12211
Research Triangle Park, NC 27709

Chief 1
Ofc of Missile Electronic Warf
Electronic Warfare Lab, ERADCOM
White Sands Missile Range, New Mexico 88002

Environmental Research Institute of Michigan 1
ATTN: IRIA Library
PO Box 618
Ann Arbor, MI 48107

DISTRIBUTION LIST (Continued)

Advisory Group on Electron Dev ATTN: Secy, Working Group D (Lasers) 201 Varick Street New York, NY 10014	1
Commander Naval Weapons Center ATTN: Mr. R. Hintz, Code 3311 China Lake, CA 93555	1
Marconi Avionics Inc. ATTN: Mr. John Weaver 4500 N. Shallowford Road Atlanta, GA 30338	1
Honeywell Systems and Research Center ATTN: Dr. Hans Mocker 2600 Ridgway Parkway Minneapolis, Minnesota	1
United Technologies Research Center ATTN: Dr. Walt Kaminski P.O. Box 2691 West Palm Beach, Florida 33402	1
Hughes Aircraft Company ATTN: Mr. Lowell Hill Laser Systems Division Centinela Avenue and Teal Street Culver City, CA 90230	1
Raytheon Company ATTN: Mr. Al Jelalian Electro-Optics Laboratory Wayland, Massachusetts 01778	1
General Electric Company Electronics Laboratory ATTN: Dr. M. Chun Syracuse, New York 13201	1